JOURNAL OF CIVILTECH

INNOVATIONS IN CIVIL ENGINEERING AND TECHNOLOGY

YEAR: **2019** VOLUME: **1** ISSUE: **2**

EARTHQUAKE **ENGINEERING**

CONSTRUCTION MANAGEMENT **ENGINEERING**

BUILDING MATERIALS **ENGINEERING**

TRANSPORTATION **ENGINEERING**

STRUCTURAL **ENGINEERING**

GEOTECHNICAL **ENGINEERING**

e-ISSN: 2687-2129

HYDRAULIC AND WATER RESOURCES **ENGINEERING**

Journal of Innovations in Civil Engineering and Technology

Volume 1, Issue 2, Year 2019
(30.12.2019)

Journal of Innovations in Civil Engineering and Technology (JICIVILTECH)

2019, Volume 1, Issue 2

The Journal Information

Publisher: Hüseyin AKBULUT

Editor-in-Chief: Hüseyin AKBULUT

Editors: Cahit GÜRER, Gökhan GÖRHAN, Gökhan KÜRKLÜ

Field Editor: Murat HİÇYILMAZ

Secretary of Publication: Burak Enis KORKMAZ, Şule YARCI

Access: Open Access

Language of Publication: English and Turkish

Publication Frequency: Twice a year (in December and June)

Type of Publication: Peer-reviewed and periodical

e-ISSN: 2687-2129

Telephone: +90 272 2182 30 00 (2324)

E-mail: j.iciviltech@gmail.com

Webpage: https://dergipark.org.tr/tr/pub/jiciviltech

Correspondence Address: Afyon Kocatepe University, Engineering Faculty, Civil Engineering Department, Ahmet Necdet Sezer Campus, 03200, Afyonkarahisar, TURKEY.

Advisory Board of the 2nd Issue

Alan WOODSIDE, *Brunel University, United Kingdom*

Bojan ZLENDER, *University of Maribor, Slovenia*

Erol TUTUMLUER, *University Of Illinois At Urbana-Champaign, United States*

Hasan TOSUN, *Eskisehir Osmangazi University, Turkey*

Hashem R. AL-MASAEID, *Jordan University of Science and Technolog, Jordan*

Hüseyin Yılmaz ARUNTAŞ, *Gazi University, Turkey*

Imad L. AL-QADI, *University Of Illinois At Urbana-Champaign, United States*

İlhami DEMİR, *Kırıkkale University, Turkey*

İsmail DEMİR, *Afyon Kocatepe University, Turkey*

João Pedro SILVA, *Polytechnic Institute of Leiria, Portugal*

Masayasu OHTSU, *Kyoto University, Japan*

Mehmet SALTAN, *Süleyman Demirel University, Turkey*

Meor Othman HAMZAH, *University Sains Malaysia, Malaysia*

Mujib RAHMAN, *Brunel University, United Kingdom*

Iqbal KHAN, *King Saud University, Saudi Arabia*

Özcan TAN, *Konya Technical University, Turkey*

Serdal TERZİ, *Süleyman Demirel University, Turkey*

Dunja PERIC, *Kansas State University, United States*

Murat KANKAL, *Uludağ University, Turkey*

Paula FOLINO, *University of Buenos Aires, Argentina*

Roumiana ZAHARIEVA, *University of Architecture, Bulgaria*

Sri Atmaja P. ROSYIDI, *Muhammadiyah University of Yogyakarta, Indonesia*

Ivanka NETINGER, *University of Osijek, Croatia*

Veli BAŞARAN, *Afyon Kocatepe University, Turkey*

Ahmet Raif BOĞA, *Afyon Kocatepe University, Turkey*

Reviewer List of the 2nd Issue

Bekir AKTAŞ, *Erciyes University, Turkey*

Ekinhan ERİŞKİN, *Süleyman Demirel University, Turkey*

Fatih ERGEZER, *Süleyman Demirel University, Turkey*

Jülide ÖNER, *Usak University, Turkey*

Mehmet AVCAR, *Süleyman Demirel University, Turkey*

Mehmet SALTAN, *Süleyman Demirel University, Turkey*

Meltem SAPLIOĞLU, *Süleyman Demirel University, Turkey*

Murat HİÇYILMAZ, *Afyon Kocatepe University, Turkey*

Murat Vergi TACİROĞLU, *Mersin University, Turkey*

Nihat MOROVA, *Isparta University of Applied Sciences, Turkey*

Serdal TERZİ, *Süleyman Demirel University, Turkey*

Veli BAŞARAN, *Afyon Kocatepe University, Turkey*

Contents / İçindekiler

JOURNAL OF JICIVILTECH
INNOVATIONS IN CIVIL ENGINNERING AND TECHNOLOGY

e-ISSN 2687-2129
jiciviltech, 2019, 1(2), *57-63*

Araştırma Makalesi / Research Article

Mathematical Modelling of Airport Pavement Layer Thickness

*[1]Ekinhan ERİŞKİN, [2]Serdal TERZİ, [3]Burak KÜÇÜKÇAPRAZ

[1]*Süleyman Demirel University, Engineering Faculty, Civil Engineering Department, Isparta, Turkey, ekinhaneriskin@sdu.edu.tr, ORCID ID: https://orcid.org/0000-0002-0087-0933*
[2]*Süleyman Demirel University, Engineering Faculty, Civil Engineering Department, Isparta, Turkey, serdalterzi@sdu.edu.tr, ORCID ID https://orcid.org/0000-0002-4776-824X*
[3]*Süleyman Demirel University, Technical Education Faculty, Building Training Department, Isparta, Turkey, acroubik@gmail.com, ORCID ID https://orcid.org/0000-0002-2548-2136*

Geliş / Recieved: 12.12.2019; Kabul / Accepted: 27.12.2019

Abstract

In this study, a mathematical model has been developed in order to avoid possible chart and reading errors of the abacas used to determine the thickness of the airport concrete pavement slab layer. The least squares method was used for the established model. R^2 was calculated as 0.91 in the model developed with 1450 abaca reading data obtained by the literature. Because of the study, it was observed that the model established to determine the thickness of airport concrete pavement slab layer has a high regression coefficient. With the developed model the thicknesses of the layer were modelled with an average error of 3.5% using the strength in psi unit of the concrete used for the pavement, the subgrade reaction modulus coefficient, the number of takeoffs per year and the design plane weight parameters.

Keywords: *Airport pavement design, Least squares method, Concrete layer thickness.*

*[1]Sorumlu yazar / Corresponding author

Bu makaleye atıf yapmak için/To cite this article
Erişkin, E., Terzi, S., & Küçükçapraz, B. (2019). Mathematical planning of airport pavement layer thickness. *Journal of Innovations in Civil Engineering and Technology (JICIVILTECH), 1*(2), 57-63.

Havaalanı Üstyapı Tabaka Kalınlıklarının Matematiksel Olarak Modellenmesi

Öz

Bu çalışmada, havaalanı üstyapı beton plak tabaka kalınlıklarının belirlenmesi amacıyla kullanılan abakların olası abak ve okuma hatalarının önüne geçmek amaçlı olarak matematiksel bir model geliştirilmiştir. Kurulan model için en küçük kareler yönteminden faydalanılmıştır. Literatür tarafından elde edilen 1450 abak okuma verileri ile birlikte kurulan modelde R^2 0.91 olarak hesaplanmıştır. Yapılan çalışma sonucunda havaalanı üstyapı beton plak tabaka kalınlıklarını belirlemek için kurulan modelin yüksek bir regresyon katsayısına sahip olduğu görülmüştür. Elde edilen model ile birlikte; havaalanı üstyapısı için kullanılan betonun psi biriminden dayanımı, doğal zemin yatak katsayısı, yıllık kalkış sayısı ve tasarım uçak ağırlığı parametrelerine bağlı olarak beton plak tabaka kalınlıkları ortalama %3.5 hata ile modellenebilmiştir.

Anahtar kelimeler: *Havaalanı üstyapı tasarımı, En küçük kareler yöntemi, Beton plak tabaka kalınlığı.*

1. Introduction

Airport pavement are very important buildings since very expensive air vehicles use them. Any deflection on the pavement can cause a very serious crash. Therefore, the pavement's parameter should be calculated correctly and the pavement should build without any mistake. The vehicles using the pavement are very heavy objects and therefore rigid pavements are preferred.

During the 1st World War, the importance of the airport pavement design method has been increased. To take off and land the planes, paved ground is needed. So, the highway pavements are used after the needed tests. When the planes weight increased, the pavement type changed to rigid pavement. To design the thickness of the pavement, airport pavement design graphs are obtained based on plane weights, gear geometries, environmental factors and grounds specifications (Okur, 2008; Yoder & Witczak, 1975).

Airport pavement design methods are divided into two methods: (*i*) empirical and (*ii*) analytical. The empirical methods are based on experience and experimental test results. Based on these, tables, charts and graphs are prepared to determine the thickness of the pavement slab layer. Analytical methods instead, take into account especially the mechanical properties of the materials used for the construction, in addition the estimated traffic load and environmental conditions, and based on these parameters, the slab layer thickness is obtained with the help of a computer program (Okur, 2008).

The oldest known design method is the CBR method. The design method changed in time like Portland Cement Association (PCA), Canadian Department of Transportation (CDOT), Federal Aviation Administration (FAA) methods (Okur, 2008; Kök, 2008). Nowadays, the development of the design method more shifted to artificial intelligence. For example, Küçükçapraz (2019) in his thesis, used fuzzy logic to determine the airport pavement slab layer thickness.

Any abaca to determine the layer thickness is very useful. However, while using the abaca, there can occur some possible mistakes because of the abaca plotting mistakes or while reading the abaca. In addition, it is very time consuming and needs a lot of attention. Therefore, Küçükçapraz's (2019) study is very useful because the probability of occurrence of the mistakes are reduced. Nevertheless, it still takes time to train and use it. Moreover, it needs many data.

This study focusses on the development of a mathematical formula for calculating the layer thickness of the airport pavement slab. Therefore, the data set of the Küçükçapraz's (2019) thesis are used. As a result, a global useable formula is obtained.

2. Data Set and Method

2.1. Data set

The data used for this study is obtained from Küçükçapraz (2019) thesis. The data set consists of five parameters. Four of them were used as input parameter and the last one, as the output parameter, was the slab layer thickness. The input and output parameters are obtained using the single wheel gear abaca (Figure 1) reading. The abaca seen in Figure 1 start with determining the concrete's flexural strength (1 psi is equal to 6.89 kPa). After determining the strength, the subgrade reaction modulus coefficient (1 pci is equal to 271.45 kN/m^3) is obtained by drawing a straight line to right. When the coefficient is obtained, a straight line to up or down based on the plane weight (1 lbs is equal to 0.45 kg) is drawn. Last of all, a straight line to right is drawn till the annual departure line is crossed. Moreover, the reading obtained at last is the slab layer thickness (1 in is equal to 2.54 cm).

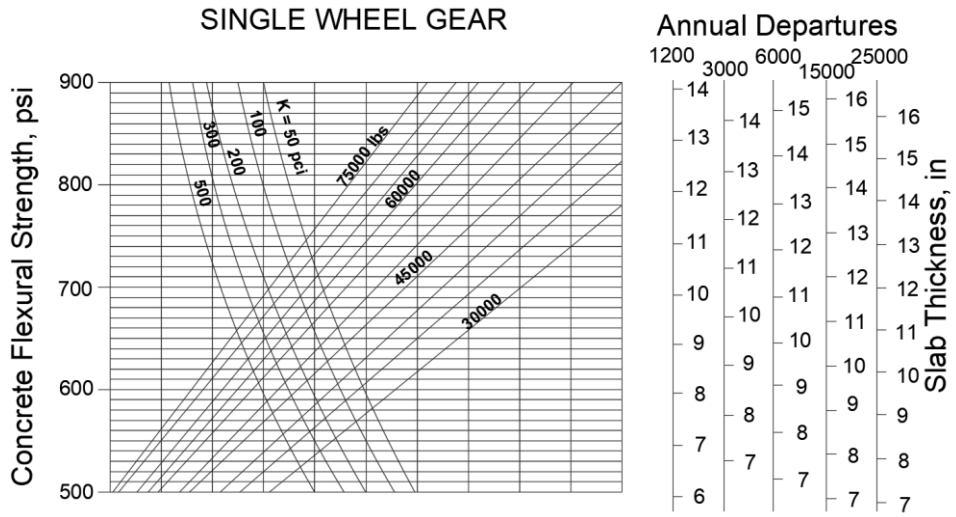

Figure 1. Slab thickness determining abaca for single wheel gear (FAA, 1995)

To create the data set, the concrete strength value is random selected between 500 and 900. The ground coefficient is random selected between 50 and 500. 10 different design plane weights are determined and used as 13620, 15890, 18160, 20430, 22700, 24970, 27240, 29510, 31780 and 34050 kg. Last of all five different annual departure counts are used as readable from the abaca as 1200, 3000, 6000, 15000 and 25000. All the created data is random combined and 1450 random selected data set is obtained by Küçükçapraz (2019). 80% of the obtained data set were used as training data and the rest 20% were used for testing data. In this study, the mathematical model is also developed based on the Küçükçapraz's (2019) training data and tested using the test data set. To develop of the mathematical model, least squares method is used.

2.2. Least squares method

Estimation methods are generally based on mathematical and statistical methods. Tendency analysis is the expression of the trend defined as the long-term trend of a time series with a line or a curve (Yalçınöz et al., 2000). Here the trend of a data set is obtained based on least squares method. Least squares method aims to find the best solution by minimising the sum of the squares of the errors (Equation 1).

$$S = \sum_{i=1}^{n}(y_i - \hat{y}_i)^2 \quad (1)$$

Where, S is the sum of the errors square, y_i is the real data and $\hat{y}_i$ is the obtained data (Chapra & Canale, 2003; Akdeniz, 2002). In this study, the linear approach given below is used. The linear approach based on that the relation between the variables and can be formulated using Equation 2 (Chapra & Canale, 2003; Akdeniz, 2002; Hengirmen, 1999).

$$y = ax + b \quad (2)$$

When the least squares method is used to zero the error than the Equation 3 and 4 is obtained. In addition, by solving the equations, the a and b coefficients can be obtained.

$$an + b\sum_{i=1}^{n} x_i = \sum_{i=1}^{n} y_i \quad (3)$$

$$a\sum_{i=1}^{n} x_i + b\sum_{i=1}^{n} {x_i}^2 = \sum_{i=1}^{n} x_i y_i \quad (4)$$

3. Mathematical Model

The slab layer thickness can be obtained based on (*i*) design plane characteristics, (*ii*) annual departures, (*iii*) concrete flexural strength and (*iv*) subgrade reaction modulus coefficient (Bayram, 2006).

When the abaca in Figure 1 examined, concrete flexural strength, plane weights, annual departures and layer thickness are linear. However, the subgrade reaction modulus is polynomial. So, the main form of the excepted formula is shown in Equation 5.

$$y = \begin{Bmatrix} a_0 + a_1x_1 + a_2x_2 \\ +{a_3}^2x_2 + {a_4}^3x_2 + a_5x_3 + a_6x_4 \end{Bmatrix} \quad (5)$$

Where, y is the layer thickness in cm, x_1 is the concrete flexural strength in psi, x_2 is the subgrade reaction modulus in pci, x_3 is the plane weights in kg and x_4 is the annual departure counts. $a_i\ \{i = 0 \dots 6\}$ is the coefficients. As mentioned above, because subgrade reaction modulus is polynomial, the coefficient is third order polynomial predicted. With the help of EXCEL software's solver tool, the least squares method was able to be applied. As a result, Equation 6 is obtained for calculating the layer thickness.

$$y = \begin{Bmatrix} 24.747 - 0.019x_1 - 0.03x_2 \\ +0.0719^2x_2 + 0.2305^3x_2 \\ +0.0005x_3 + 0.0001x_4 \end{Bmatrix} \quad (6)$$

As seen from Equation 6, annual departure counts have the less impact on the layer thickness. The comparison of the calculated thickness values using Equation 6 and obtained thickness values from abaca are shown in Figure 2 and 3.

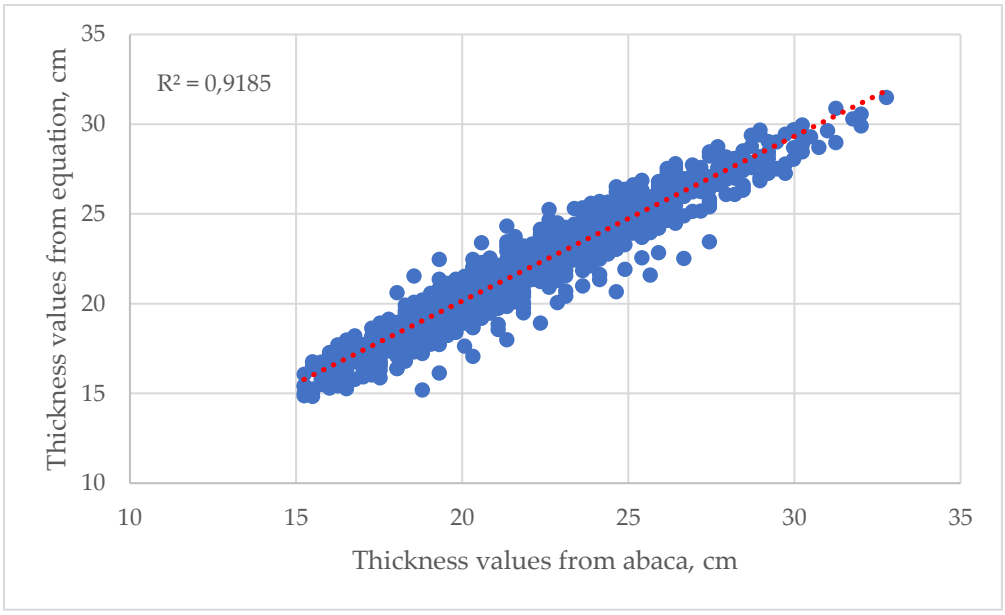

Figure 2. The regression value between calculated and abaca obtained thickness values for training data set

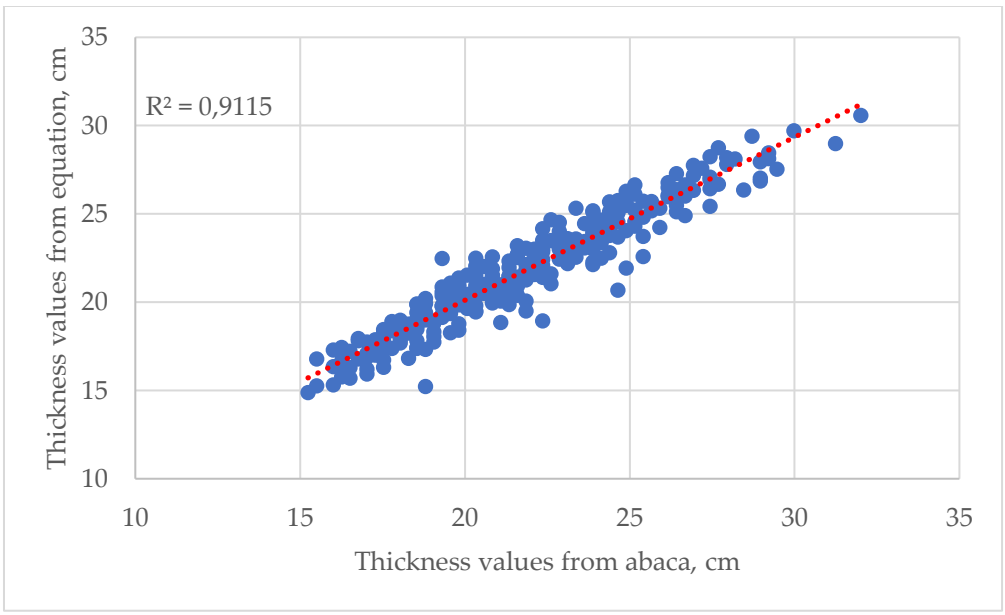

Figure 3. The regression value between calculated and abaca obtained thickness values for test data set

As seen in Figure 2 and 3, the thickness values are close to values obtained by abaca reading. In addition, for both, training and test data set, the regression between the data are very high, ~91%. Last of all, the error obtained from calculation has an average of 3.5% which is very low.

4. Conclusion

In this study, it is focused on developing a novel mathematical equation to calculate the layer thickness based on concrete flexural strength, plane weights, annual departures and subgrade reaction modulus. There is some abaca to determine the layer thicknesses but it is both time consuming and easy to make mistakes. So, suggesting a mathematical model can handle these handicaps.

For developing the equation, data set of Küçükçapraz (2019) has been used. As a result of the development, thickness values got close to the abaca read thickness values with a regression coefficient of 91.85%. After developing the equation using the training data set, the equation attempted for the test data set. Also using the equation for these data set gave a high regression value of 91.15%. The average mistake was 3.5% which is very low. So, the developed mathematical model could be used to determine the slab layer thickness for airport pavements.

5. References

Akdeniz, F. (2002). *Olasılık ve İstatistik*. Baki Kitabevi.

Bayram, A. (2006). *Hava alanları pist dolgularının geosentetik malzemeler kullanılarak güçlendirilmesi.* Yüksek Lisans Tezi. İstanbul Teknik Üniversitesi, İstanbul.

Chapra, S. C., & Canale, R. P. (2003). *Mühendisler için Sayısal Yöntemler*. Literatür Yayıncılık.

Federal Aviation Administration, (1995). Advisory Circular, AC No: 150/5320-6D–7.7.95, Airport Pavement Design and Evulation.

Hengirmen, M. O. (1999). Comparison of three forecast methods for power demand in Gaziantep. *ELECO'99*. Bursa, Turkey.

Kök, E. (2008). *Karayolu ve havaalanı üstyapı tasarım yöntemleri, karşılaştırması ve Türkiye uygulamaları*. Yüksek Lisans Tezi. İstanbul Teknik Üniversitesi, İstanbul.

Küçükçapraz, B. (2019). *Havaalanı üstyapılarının yapay zeka yöntemleri ile planlanması.* Yüksek Lisans Tezi. Süleyman Demirel Üniversitesi, Isparta.

Okur, F. (2008). *Havaalanı üstyapı tasarım yöntemleri*. Yüksek Lisans Tezi. İstanbul Teknik Üniversitesi, İstanbul.

Yalçınöz, T., Karadeniz, Y., & Yücel, İ. (2000). Niğde bölgesi için elektrik yük tahmini. *ELECO'2000.* Bursa, Turkey.

Yoder, E. J., & Witczak, M. W. (1975). *Principles of Pavement Design*. U.S.A.: John Wiley & Sons, Inc.

JOURNAL OF JICIVILTECH
INNOVATIONS IN CIVIL ENGINNERING AND TECHNOLOGY

e-ISSN 2687-2129
jiciviltech, 2019, *1*(2), 65-74

Araştırma Makalesi / Research Article

Karbon Siyahı Katkılı Bitümlerin Taş Mastik Asfalt Karışımlarda Elektriksel İletkenlik Özelliklerine Olan Etkisinin Araştırılması

*[1]Cahit GÜRER, [2]Ayfer ELMACI

[1]Afyon Kocatepe Üniversitesi, Mühendislik Fakültesi, İnşaat Mühendisliği Bölümü, Afyonkarahisar/Türkiye, cgurer@aku.edu.tr, ORCID ID: https://orcid.org/0000-0003-1413-2357
[2]Afyon Kocatepe Üniversitesi, Emirdağ Meslek Yüksekokulu, İnşaat Bölümü, Yapı Denetimi Programı, Afyonkarahisar/Türkiye, aelmaci@aku.edu.tr, ORCID ID: https://orcid.org/0000-0001-7939-0002

Geliş / Recieved: 14.12.2019; Kabul / Accepted: 28.12.2019

Öz

Geleneksel bitümlü karışımlar yalıtkan bir özellik göstermektedir bununla birlikte bu tip bitümlü sıcak karışımların iletkenliği karışım içerisine iletken malzemeler ilave edilerek geliştirilebilir. Bu malzemeler bitümlü bağlayıcının içeriğine toz orak eklenen iletken maddeler olabileceği gibi agregaya eklenen iletken lif ve cüruf gibi maddeler de olabilir. Yalnızca agrega, karbon lifi ve karbon siyahı gibi katkılarla iletken bitümlü karışımlar oluşturulabilir. Fakat asfalt karışımlardaki bitüm miktarı arttıkça iletkenlik özelliğinde azalma meydana gelir. Bu durum özellikle içeriğindeki bitüm miktarı yüksek olan taş mastik asfalt (TMA) gibi bitümlü karışımlarda problem oluşturur. Genellikle taş mastik asfalt karışımlar karayollarının köprü ve tünel gibi kesimlerinde sıklıkla tercih edilmektedir. Bu çalışma kapsamında laboratuvarda 3 farklı seri olarak hazırlanmış TMA numunelerinde elektriksel iletkenlik özellikleri, özdirenç ve sabit elektrik gerilimi (20 Volt) ile Isıtma deneyleri sonucunda bulunan değerler karşılaştırılmış ve TMA karışımlarda karbon lifinin elektriksel özelliklerin geliştirilmesinde oldukça etkili olduğu görülmüştür.

Anahtar kelimeler: *Elektriksel iletkenlik, Taş mastik asfalt (TMA), Karbon siyahı, Karbon lifi, Buzlanma önleme.*

*[1]Sorumlu yazar / Corresponding author

Bu makaleye atıf yapmak için
Gürer, C., & Elmacı, A. (2019). Karbon siyahı katkılı bitümlerin taş mastik asfalt karışımlarda elektriksel iletkenlik özelliklerine olan etkisinin araştırılması. *Journal of Innovations in Civil Engineering and Technology (JICIVILTECH)*, *1*(2), 65-74.

Investigation the Effect of Carbon Black Additive Bitumen on Electrically Conductivity Properties of Stone Mastic Asphalt Mixtures

Abstract

Conventional bituminous mixtures have insulating properties, although the conductivity of such bituminous hot mixtures can be improved by adding conductive materials into the mixture. These materials may be conductive materials added to the contents of the bituminous binder, such as dust, sickles, conductive fibers and slag added to the aggregate. Conductive bituminous mixtures can only be formed with additives such as aggregate, carbon fiber and carbon black. However, as the amount of bitumen in the asphalt mixes increases, the conductivity decreases. This situation creates problems especially in bituminous mixtures such as stone mastic asphalt (SMA) with high bitumen content. Stone mastic asphalt pavements are frequently applied in sections such as bridges and tunnels where icing occurs most rapidly. In this thesis, electrical conductivity properties, resistivity and heating via constant electric voltage (20 Volt) tests results were compared with the samples prepared in 3 different series and it was concluded that the carbon fiber was found to be highly effective in the development of electrical properties in the SMA mixtures.

Keywords: *Electrical conductivity, Stone mastic asphalt (SMA), Carbon powder, Carbon fiber, Anti-icing.*

1. Giriş

Kış aylarındaki kar, buz fırtınası, buzlanma vb. etkiler karayolu ulaşımında önemli problemlere neden olmakta özellikle köprü, tünel ve düşey kurp gibi yol kesimlerinde trafik sıkışıklığına ve havalimanlarında uçuş iptallerine neden olabilmekte bu da büyük maddi ve manevi kayıplara yol açmaktadır (Liu, Wu, Ye, Qiu, & Li, 2008; Wu, Mo, Shui, & Chen, 2005). Bundan dolayı yol yüzeyindeki kar ve buzlanmanın zamanında kaldırılması ve yolun güvenli bir şekilde trafiğe açılması geçmişten bu yana en çok ilgi duyulan konuların başında gelmektedir (García, Schlangen, van de Ven, & Liu, 2009; Minsk, 1968). Özellikle karlı ve buzlanmanın olduğu havalarda, yüksek taşıt hızlarında yol yüzeyi ile tekerlek bandajı arasında oluşan sürtünme direnci çok küçük değerlere inebilmektedir. İngiltere'de yapılan bir çalışma kaplamanın kayma direnci değerinde %10'luk bir iyileştirmenin, yağışlı havalarda meydana gelen trafik kazalarında %13'lik bir azalma sağladığını ortaya koymuştur (Gürer, Düşmez, Boğa, & Akbulut, 2019; Gürer, Düşmez, & Demirci, 2015). Buzlanma ile zamanında müdahale sonucu trafik kazaların engellenmesi ve azaltılması, ileriye dönük büyük bir maddi -manevi kazanım olacaktır. Karayollarında buzlanma ile mücadelede acil eylem planı yetersiz olan yerel yönetimler ve yol idareleri bu tip olağanüstü hava koşullarına yeterince hızlı müdahale edememektedirler. Kimyasal madde ve tuz kullanımı, görünüşte düşük maliyetli bir çözüm olarak görülmekte bununla birlikte yalnızca hava sıcaklığının çok düşük olmadığı şartlarda fayda sağlamaktadır (Ağar & Kutluhan, 2005). Köprüler, karayollarının yatay ve düşey kurp kesimleri, yonca kavşaklar, tüneller ve hastane acil servis ulaşım yolları, kaldırımlar vb. yol kesimleri kar birikmesi ve buzlanma açısından en kritik kesimleri oluşturmaktadır. Özellikle köprü ve tünel gibi yol kesimlerinde, yüksek yük taşıma kapasitesi, daha uzun ömürlü oluşu ve daha az bakım gerektirmelerinden dolayı taş mastik asfalt (TMA) karışımlar tercih edilmektedirler. Asma köprü ve tünel gibi karayolu geçişleri buzlanmanın diğer yol kısımlarına göre daha gerçekleştiği kesimlerdir. Özellikle köprüler her yönden hava şartlarına açık yapılar olduğu için köprülerde buzlanma, normal yol kesimlerine göre daha hızlı meydana gelir (Şekil 1).

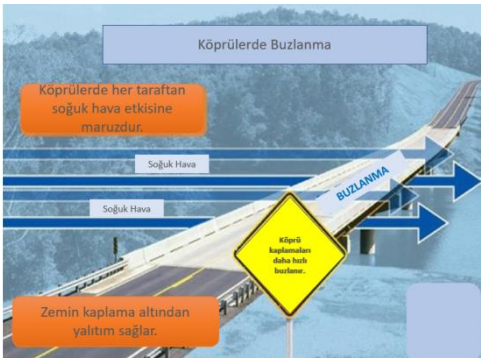

Şekil 1. Köprülerde buzlanma (Shepherd, 2017).

Geleneksel olarak kullanılan, kimyasal solüsyon ve tuz uygulama gibi buzlanma ile mücadele yöntemleri köprü gibi yapıların metal ve betonarme taşıyıcı sistemlerine zarar vererek, telafisi güç durumlara neden olabilirler. Bundan dolayı bu gibi kesimlerde son

yıllarda iletken kablo ile kaplama ısıtma sistemleri, asfalt ve solüsyon püskürtme gibi sistemler giderek artan oranlarda uygulanmaya başlamıştır (Gürer et al., 2015). Köprü kaplamaları TMA karışımlardan oluştuğu için yüksek bitüm yüzdesi elektriksel iletkenlik özelliği üzerinde azaltıcı etki yapmaktadır. Dolayısıyla TMA gibi bitümlü karışımları elektriksel iletken hale getirmede bitüm fazının da iletken olması veya iletken materyaller içermesi bu açıdan bakıldığında oldukça önemlidir. Bu sayede iletkenlik özelliği bitüm film kalınlığının artışıyla birlikte azalmamış olacaktır Bu çalışmanın literatürdeki en önemli farkı ilk kez bağlayıcı fazının da iletkenliğe katkıda bulunan TMA karışımlardan oluşmasıdır (Gürer & Gürgöze, 2017). Bu çalışmada TMA karışımlarda bitüm yüzdesi artışıyla iletkenliğin azalmasını önlemek için karbon siyahı katkılı bitüm numunesi hazırlanarak bu bağlayıcı ile TMA karışımlar üretilmiş ve elektriksel iletkenlik üzerinde olan etkileri belirlenmiştir.

2. Materyal ve Yöntem

2.1. Materyal

Çalışmada mineral filler ve ince agrega olarak Afyonkarahisar'da faaliyet gösteren KOLSAN AŞ'den temin edilmiş kireçtaşı ve iri agrega olarak Kütahya Bölgesinden temin edilmiş bazalt kökenli agrega kullanılmıştır. Kullanılan agregaların özellikleri Tablo 1'de verilmiştir. Bağlayıcı malzeme olarak Afyonkarahisar Asfalt üretim tesislerinden temin edilmiş B50/70 penetrasyon bitümü kullanılmış olup bitüm özellikleri Tablo 2'de verilmiştir. Ve bu bitüm ayrıca ağırlıkça %14 karbon siyahı ile 2 saat süre ile 185 ^{o}C'de, tam kesmeli bir karıştırıcıyla 1800 dev/dk hızda karıştırmak suretiyle modifiye edilmiş ve bağlayıcı olarak kullanılarak iletken TMA karışım numuneleri üretilmiştir. %14 karbon tozu miktarı halen devam eden 17.KARİYER.206 nolu AKÜ BAPK projesinin 2.ara rapor sonuçlarındaki bulgular esas alınarak belirlenmiştir (Gürer, Akbulut & Boğa, 2018). Bitümlerin modifiye edilmesinde kullanılan karbon siyahları ise ÖZERBAND Konveyor Sanayi AŞ'den temin edilmiştir. Çalışmada kullanılan üç farklı iletken TMA numune serilerine ait özellikler Tablo 3'te ve gradasyon aralıkları ise Tablo 4'de verilmiştir.

2.2. Yöntem

Çalışmanın yöntem akış şeması Şekil 2'de verilmiştir. Deneysel çalışma kapsamında TMA numuneler üzerinde iki elektrot yöntemi ile özdirenç ölçümü ve 20 Volt DC gerilim altında ısınma deneyleri yapılmıştır. Isınma deneyleri tekli ve aynı seriden ikili numunelerin birleştirilmesi ile tekrarlanmıştır.

Tablo 1. TMA karışımlarda kullanılan agrega özellikleri

Agrega Deneyleri	Kireçtaşı (İnce Fraksiyon)	Bazalt (Kaba Fraksiyon)
İri Agrega Hacim Özgül Ağırlık (>No:4) (gr/cm^3)	2,721	2,673
İri Agrega Zahiri Özgül Ağırlık (>No:4) (gr/cm^3)	2,730	2,772
İnce Agrega Hacim Özgül Ağırlık (No:4-200) (gr/cm^3)	2,186	-
İnce Agrega Zahiri Özgül Ağırlık (No:4-200) (gr/cm^3)	2,592	-
Mineral Filler Zahiri Özgül Ağırlık (<No:200) (gr/cm^3)	2,560	
Su Emme Deneyi (%) (>No:4)	0,4	4,0
Su Emme Deneyi (%) (No:4 – No:200)	4,0	8,7
Los Angeles Aşınma Kaybı (%)	23,1	15,8
Darbelenme Kaybı (%)	5,03	3,50
$NaSO_4$ Donma Kaybı (%)	0,69	7,53
Karbon Siyahı BET Yüzey Alanı (m^2/gr)	87,1492	

Tablo 2. Saf bitüm özellikleri

Özellikler	Değerler	Standartlar
Temin Edilen Rafineri	Aliağa	-
Penetrasyon Sınıfı	50/70	-
Penetrasyon (25 ^oC'de)	55,1	ASTM D5-06e1
Özgül Ağırlık	1,035	ASTM D70-09e1
Yumuşama Noktası (^oC)	49,1	ASTMD36/D36M-09
Isıtma Kaybı (%)	2,2	ASTM D6-95
Parlama Noktası (^oC)	289	ASTM D5-06e1
Düktilite (5cm/dk)	>100 cm	ASTM D113-07
Viskozite (135 ^oC) (cP)	250.0	ASTM D4402-06
Viskozite (165 ^oC) (cP)	67,8	

Tablo 3. TMA Numune serilerine ait özellikler

Seri	Karbon Lifi	%14 Karbon Siyahı Katkılı Bitüm
1	✓	
2	✓	✓
3		✓

Tablo 4. TMA Serilerinin gradasyon özellikleri

Elek Boyutu		%EG	% Kalan
inc	mm		
1	25	100	0
¾	19	100	0
½	12,5	100	0
3/8	9,5	85	15
No:4	4,75	35	65
No:10	2	25	75
No:40	0,425	17	83
No:80	0,180	13	87
No:200	0,075	10	90

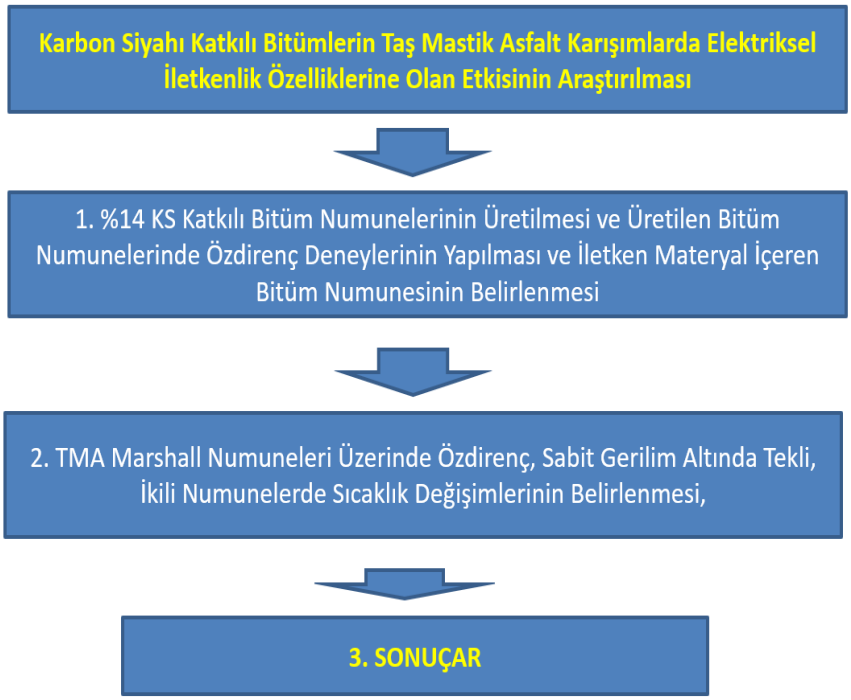

Şekil 2. Yöntem akış şeması

3. Bulgular

3.1 Özdirenç Ölçüm Sonuçları

Üretilen TMA Marshall numunelerinde %14 karbon siyahı katkılı bitümün iletkenlik üzerindeki etkisini belirlemek için tüm numunelerde iki elektrot ile dıştan temas yöntemiyle özdirenç ölçümleri yapılmıştır.

Şekil 3 ve 4'de görüldüğü gibi %14 karbon siyahı katkılı bitümle üretilen numunelerde %8,0 bitüm oranında

özdirenç değerinin 1,7 Ω.m değerine düştüğü, oldukça iyi iletken malzeme haline geldikleri görülmektedir. Yalnızca karbon lifi içeren Seri 1 numunelerine göre iki kat daha iyi iletken haline gelmişlerdir (Şekil 3). Seri 3 numunelerinde, iletken bileşen olarak, yalnızca %14 KS katkılı bitüm kullanımı TMA numunelerinin iletken hale gelmesini sağlayamamıştır. Bundan dolayı Seri 3'e ait grafik verilememiştir.

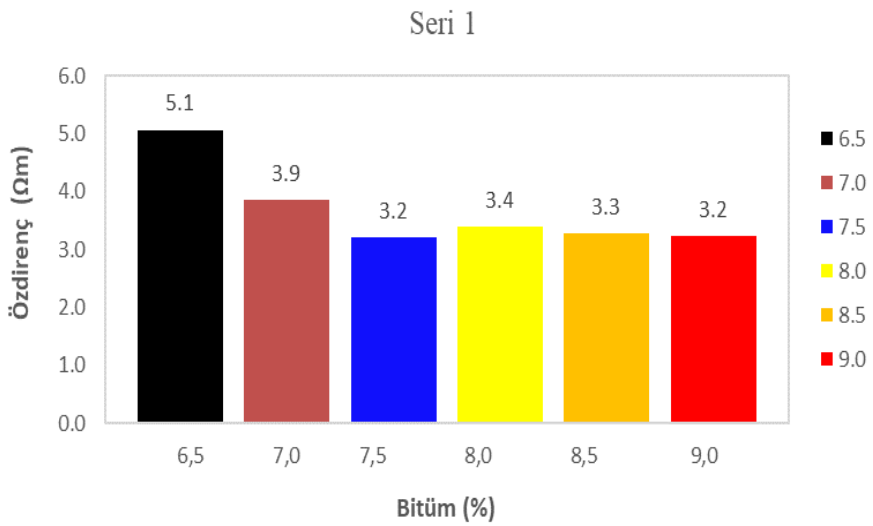

Şekil 3. Seri 1 TMA numunelerinin özdirenç değişimleri

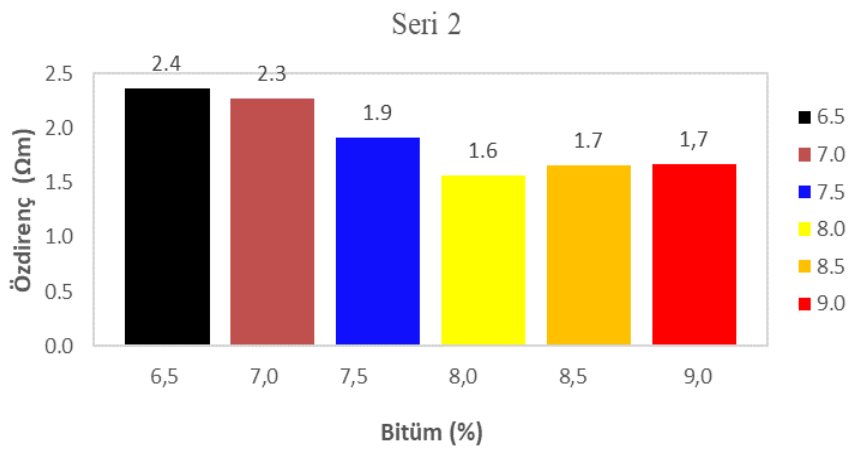

Şekil 4. Seri 2 TMA numunelerinin özdirenç değişimleri.

3.2 Sabit Gerilim Altında Tekli Numunelerin Sıcaklık Artışlarının Belirlenmesi

Bu deney kapsamında tekli numunelere 20 Volt gerilim verilerek sıcaklıklarda meydana gelen değişimler kızılötesi

termometre ile numune ortasındaki üç noktadan ölçülerek 10 dk'lık elektrik gerilimine tabi tutulan asfalt briketi numunelerindeki sıcaklık değişimleri, bitüm yüzdelerine göre, belirlenmiştir (Şekil 5).

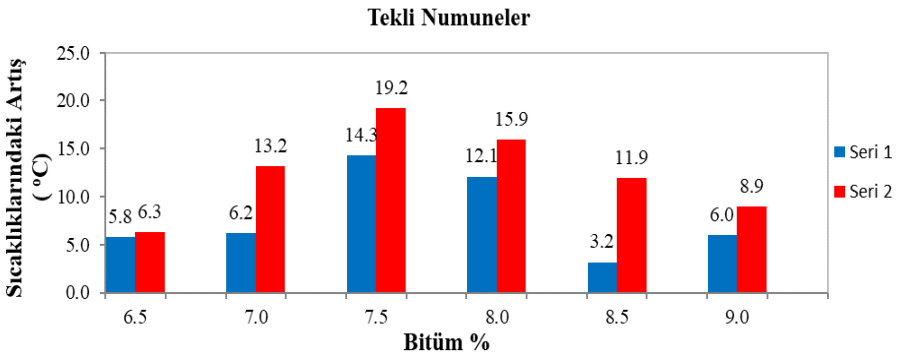

Şekil 5. Tekli TMA numunelerin sabit gerilim altında sıcaklık değişimleri

En yüksek sıcaklık artışları, Seri 1 'de %8,0 bitüm oranında 5,4 °C olarak, Seri 2 numunelerinde, %7,0 bitüm oranında 7,2 °C olarak belirlenmiştir. Her iki seriye ait numunelerde 8,0'ın üzerine çıkmasıyla numunelerde ortalama sıcaklık artışlarında azalma görülmektedir. Karbon siyahı katkılı bitümle üretilen numunelerde görülen sıcaklık artışları genel olarak Seri 1 numunelerine göre daha yüksektir.

3.3. Sabit Gerilim Altında İkili Numunelerin Sıcaklık Artışlarının Belirlenmesi

İkili numunelerde sabit gerilim altında sıcaklık artışlarını belirlemek için 30 Volt sabit DC gerilim 10 dk boyunca birbirine temas ettirilmiş numunelere uygulanmış ve numunelerdeki sıcaklık değişimleri belirlenmiştir. Numunelerin uzunlukları arttığı için direnç değeri artmış ve sıcaklık değerlerindeki artışlarda, tekli numune ölçümlerine göre azalma görülmüştür. Bununla birlikte %14 karbon siyahı katkılı bitümlerle üretilen TMA numunelerindeki (Seri 2) sıcaklık artışlarının Seri-1 numunelere göre oldukça yüksek olduğu görülmektedir. Yalnızca %6,5 bitüm oranında Seri 2 numunesindeki sıcaklık artışı düşüktür. Karbon siyahı katkılı bitümün Seri 2 numunelerinin sıcaklık artışlarının yüksek oluşunda etkili olduğu düşünülmektedir (Şekil 6).

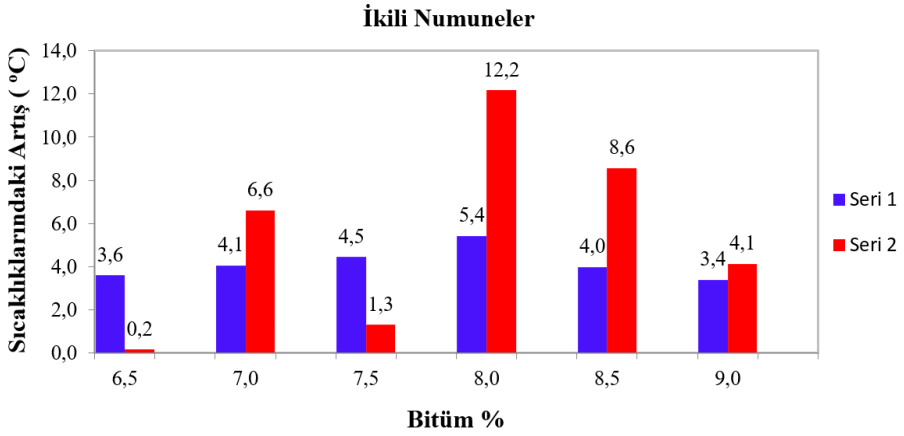

Şekil 6. İkili TMA numunelerin sabit gerilim altında sıcaklık değişimleri

4. Sonuçlar

4. Sonuçlar ve Tartışma

Yapılan deneysel çalışmalar neticesinde, şu sonuçlara ulaşılmıştır:

- Karbon siyahı katkılı bitüm kullanımı aynı gradasyon ve iletken madde içeriğine sahip TMA numunelerini iki kat daha iletken hale getirmiştir.

- Tüm numunelerde bitüm yüzdesinin artmasıyla birlikte iletkenlik değerlerinin de, bitüm türüne bakılmaksızın arttığı, fakat artış değerinin karbon siyahı katkılı bitüm kullanılan Seri 2 numunelerinde daha fazla olduğu görülmüştür. Bitüm yüzdesinin artmasıyla birlikte işlenebilirliğin artması ve bu sayede karışım içerisindeki karbon liflerinin daha homojen dağılması iletkenliğin de artmasına neden olmuştur.

- Malzemeleri iletken hale çevirmede karbon lifi en çok kullanılan ve araştırılan malzemelerin başında gelmektedir. Bununla birlikte karbon lifi oldukça pahalı bir malzemedir. Karbon siyahı katkılı bitüm kullanılarak, karışım içerisindeki karbon lifi iletken bileşeni azaltılabilir. Bu sayede iletken TMA birim maliyeti de azalmış olur.

- Özellikle köprü gibi karayollarında buzlanmanın çok daha çabuk ve hızlı olduğu kesimlerde TMA karışımlar kaplama olarak tercih edilmektedir. Bu tip yol kesimlerinde iletken TMA kullanımında karbon siyahı katkılı bitümlerle uygulama yapılması tercih edildiğinde buzlanma tehlikesiyle hiç karşılaşılmaya bilinir.

- Bundan sonraki çalışmalarda yalnızca bitüm fazı ile karışımların iletken hale

dönüştürülmesi üzerine daha detaylı araştırmalar yapılmalıdır.

Teşekkür

Yazarlar çalışmaya 17.KARİYER.206 ve 18.KARİYER.214 nolu projelerle katkı sağlayan Afyon Kocatepe Üniversitesi, Bilimsel Araştırma Projeleri Koordinasyon birimine, Özerband Konveyör San. A.Ş.'ye, KOLSAN A.Ş'ye, Afyonkarahisar Belediyesi Asfalt Üretim Tesislerine, DowAksa İleri Kompozit Malzemeler San. Ltd. Şti'ye teşekkür ederler.

5. Kaynaklar

Ağar, E., & Kutluhan, S. (2005). Karayollarında kış bakımı, kar ve buz kontrolü. *TMMOB İstanbul Bülten, 76*, 10-16.

García, Á., Schlangen, E., van de Ven, M., & Liu, Q. (2009). Electrical conductivity of asphalt mortar containing conductive fibers and fillers. *Construction Building Materials, 23*(10), 3175-3181.

Gürer, C., Düşmez, C., Boğa, A. R., & Akbulut, H. (2019). *Elektriksel iletkenlik özelliği olan asfalt betonu geliştirilmesi: Afyon Kocatepe Üniversitesi Bilimsel Araştırma Projesi Sonuç Raporu* (Rapor No. 15.MUH.14). Retrieved from http://ebap.aku.edu.tr/index.php?act=guest&act2=projeler&durum=tamam

Gürer, C., Düşmez, C., & Demirci, B. (2015). Buzlanma ile mücadelede modern yöntemler. *Elektronik Mesleki Gelişim ve Araştırma Dergisi* (EJOIR). *1*(özel sayı), 43-52.

Gürer, C., & Gürgöze, H. (2017). Investigation the characteristics of conductive asphalt concrete with carbon fibre. *International Journal of Innovative Research In Science, Engineering and Technology (IJIRSET), 6*(10), 57-63.

Gürer, C., Akbulut, H., & Boğa, A. R. (2018). *Elektriksel iletken bitümlü bağlayıcı özelliklerinin araştırılması: Afyon Kocatepe Üniversitesi Bilimsel Araştırma Projesi 2. Ara Raporu. (Rapor No. 17.KARİYER.206).*

Liu, X., Wu, S., Ye, Q., Qiu, J., & Li, B. (2008). Properties evaluation of asphalt-based composites with graphite and mine powders. *Construction Building Materials, 22*(3), 121-126.

Minsk, L. D. (1968). Electrically conductive asphalt for control of snow and ice accumulation. *Highway Research Record* (227).

Shepherd, M. (2017, December 19). *The science behind why bridges ice before roads.* Retrieved September 20, 2019, from https://www.forbes.com/sites/marshallshepherd/2017/12/19/the-science-of-why-bridges-ice-before-roads/#705f470c7cd0

Wu, S., Mo, L., Shui, Z., & Chen, Z. (2005). Investigation of the conductivity of asphalt concrete containing conductive fillers. *Carbon, 43*(7), 1358-1363.

JOURNAL OF JICIVILTECH
INNOVATIONS IN CIVIL ENGINNERING AND TECHNOLOGY

e-ISSN 2687-2129
jiciviltech, 2019, 1(2), *75-97*

Araştırma Makalesi / Research Article

Pretensioning Cable Roof Systems Besiktas Stadium Design Principles

*[1]Selçuk İZ

[1]*Yeditepe Üniversitesi, Mühendislik Fakültesi, İnşaat Mühendisliği, İstanbul, Türkiye, selcukiz@yahoo.com.tr,*
ORCID ID: http://orcid.org/0000-0003-2163-8313

Geliş / Recieved: 17.12.2019; Kabul / Accepted: 28.12.2019

Abstract

In this study, design criteria of Besiktas Inonu Stadium, and the roof with a prestressed rope system, are included. Selection of systems in these structures, determination of the loads affecting the structure, analysis and design procedures of structural elements are explained. The geometry of the stadium structure, the assumptions made in the model for static and seismic analysis of the structure and the details of the analysis model are presented with this article. the necessity of building a rope roof system consists of a summary of mathematical models for the design criteria of the roof. For the roof design of this stadium which basically takes the mechanical working principle of a bicycle wheel as a starting point, the minimization and behavior modeling of the horizontal loads which can be transferred from the roof to the structure in a possible earthquake are summarized in this article including the wind tunnel test.

Keywords: *Cable, Prestressed steel, Ring beam, Membrane roof.*

*[1]Sorumlu yazar / Corresponding author

Bu makaleye atıf yapmak için
İz, S. (2019). Pretensioning cable roof systems Besiktas stadium design principles. *Journal of Innovations in Civil Engineering and Technology (JICIVILTECH), 1*(2), 75-97.

Öngerilmeli Halatlı Çatı Sistemleri Beşiktaş Stadı Tasarım Kriterleri

Öz

Bu çalışmada halatlı çatı sistemi ile inşa edilmiş Beşiktaş İnönü Stadı tasarım kriterlerine yer verilmiştir. Bu tür yapılarda taşıyıcı sistem seçimi, yapıya etkiyen yüklerin belirlenmesi ile yapısal elemanların analiz ve tasarım prosedürleri açıklanmıştır. Stadyum yapısının geometrisi Yapının statik ve depremli durum analizi için oluşturulan sonlu elemanlar modelinde yapılan kabuller ve analiz modeli ile ilgili detaylarda bu makale kapsamında sunulmuştur. Çatı geometrisinde uyulması gerekli kriterler halatlı çatı sistemi yapılması gerekliliği matematik modellerin özetinden oluşmaktadır. Bisiklet tekerleği mekanik çalışma prensibini örnek alan stadın çatı sistemi tasarımında öngerilmeli halatlı çatıların çatı ring kirişi ve üstten ankastre aşağıdan mafsallı kolon elemanları kullanılarak olası bir depremde çatıdan aktarılacak yatay yüklerin minimizasyonu ve davranış modellemesi özetlenmiştir. Ayrıca çatı ve üzerine oturduğu betonarme stad yapısı arasındaki dinamik karekteristikleri yansıtan çalışma rüzgar tünel testi sonuçları özet halinde verilmiştir.

Anahtar kelimeler: *Kablo, Öngerilmeli çelik, Halka kirişi, Membran çatı.*

1. Introduction

The Besiktas Vodafone Arena is located in Istanbul, Turkey. The general view and typical section of the stadium are shown in Figures 1 and 2. The building is oriented along two main axes and rotated by 36.4° to the cardinal directions. The primary building structure of the project consists of concrete grandstands to provide the support for a lightweight roof which covers the full perimeter of the stadium, as well as a part of the inner area. The footprint of the roof structure is approximately 216 m long and 161 m wide. The roof is divided to 42 transversal bays, whereas concrete work is divided into 86 axes, including 4 twin axes at the movement joints. The roof is a cabled structure which is completed with 1 central Lower Tension Ring, 3 central Upper Rings and 1 compression ring. Radially, the roof is sloped approx. 4° upwards. The roof will be covered primarily by a lightweight textile membrane made of Silicon coated glass fiber. TS500, TS498, Earthquake Regulation in the design of the stadium structure. Eurocode, AISC, ACI 318-02, NEHRP 2003, etc. have been used from many international regulations other than local regulations.

Figure 1. Stadium general view.

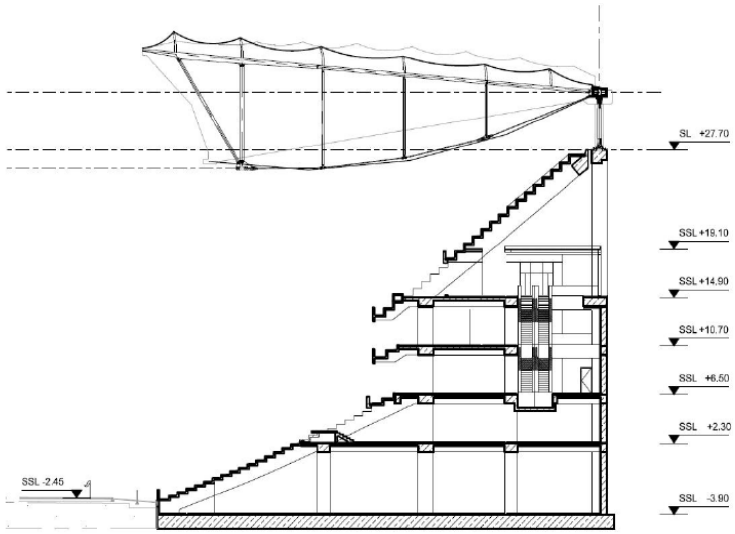

Figure 2. Stadium typical section

2. Geometry of Structural System

Structurally, the inner part of the Roof includes a T-structure made for the Lower Tension Ring, a Flying Column, and the last two elements of the Upper Radials, which holds the three Upper Rings, as well as an Inclined Strut. The T-Structure is pre-assembled before the Big Lift. The Compression Ring rests on 86 steel Columns, which are pinned radially to the concrete structure and bolted to the Compression Ring (Figure 3).

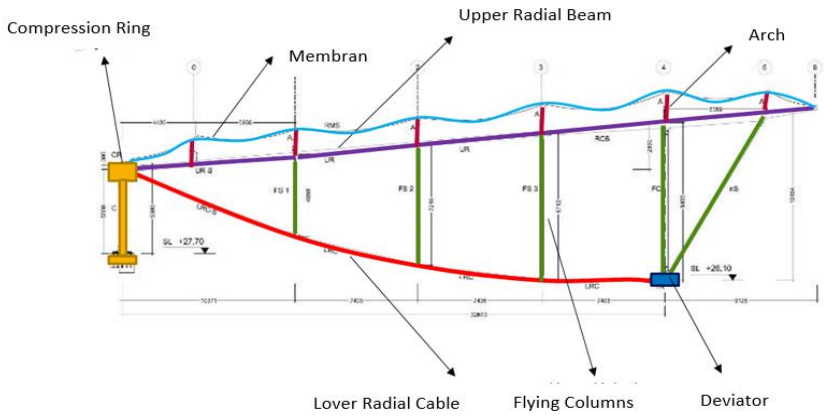

Figure 3. Besiktas stadium typical structure system.

The Compression Ring is approx. 630 m long and consists of three main parts, due to the oval shape of the roof. The central Rings (Upper and Lower) are tied to the Compression Ring by Radial elements, approx. 9 m long. As the columns are double than the number of bays, the Radial elements are split at the end. The inner Upper Ring is connected to the rest of the roof with cantilevering Upper Radials and to the Flying Columns. Due to the span of the cantilevers (approx. 9 m) intermediate supports are required between the flying columns and the tips (Inclined Struts). The Lower Tension Ring is connected to the Compression Ring with Lower Radial Cables, while the Upper Rings are connected with Upper Radial bending stiff elements. Upper and Lower radials re connected together via Flying Struts (length variable from 4 to 8 m) and Flying Columns, approx. 9 m long. Upper Radials support the membrane Arches, which are connected to the roof planes. The membrane has a typical span of ~10 m between arches and 10~15 m along arch span. At each axis, Lower Radial Cables have different curvatures, depending on the global in plane stiffness of the structure and in particular of the Compression Ring: where the Compression Ring has a small curvature because the system needs to become softer. The Lower Radial Cables have a bigger curvature, while the Compression Ring has a small curvature to ensure that the Lower Radials to become straight. The mathematical model of the stadium is shown in Figure 4.

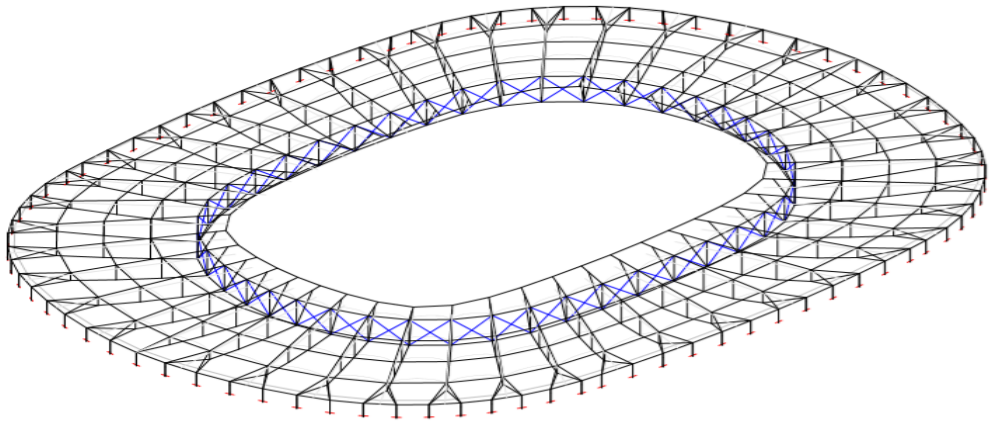

Figure 4. Besiktas Stadium mathematical model.

3. Principle of a Spoked Wheel System

It is known from engravings and old paintings that the roof covering similar to the first bicycle wheel technology known in history was used in Rome-Collosseum in ancient times (Figure 5). This system is thought to be the radial ropes that stretch the sail rope that

cannot form the core and the sail cloth covering it (Masubuchi, 2012).

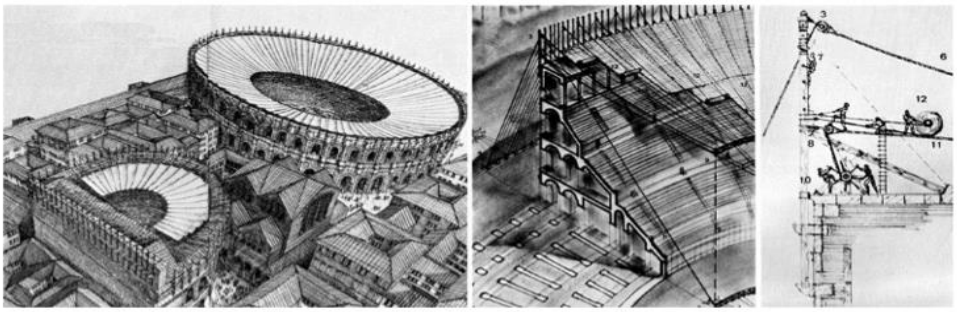

Figure 5. Engraving of the first application; Collosseum-Rome

In the system consisting of pressure and pull ring and radial ropes connecting them, the pull ring and the pressure ring forces are fixed to the pressure ring by radial ropes. This system can be briefly described as follows. The outer pressure ring or rings are fixed to the roof or the ground. With the radial ropes, the towing ring is tensioned and connected to the outer pressure ring.

The tensile force (V) in this radial cable is given in the following figure. (S) is the sum of the tensile force formed in the pull ring. If the vertical (dead + live) load (P) is applied to this structure, it is carried by the prestressing force in the cable. The load from the prestressing force must always be higher than the load (Bergermann & Chlaich, 1992).

In the world, one or two pressure rings are generally used in the applications of this system. A single pressure ring was used in Besiktas stadium.

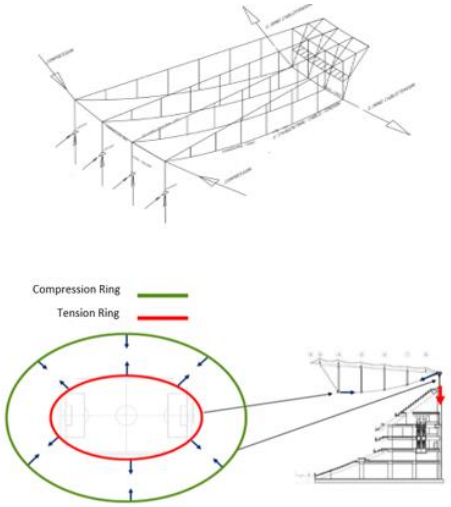

Figure 6. Typical load flow of besiktas stadium structural system.

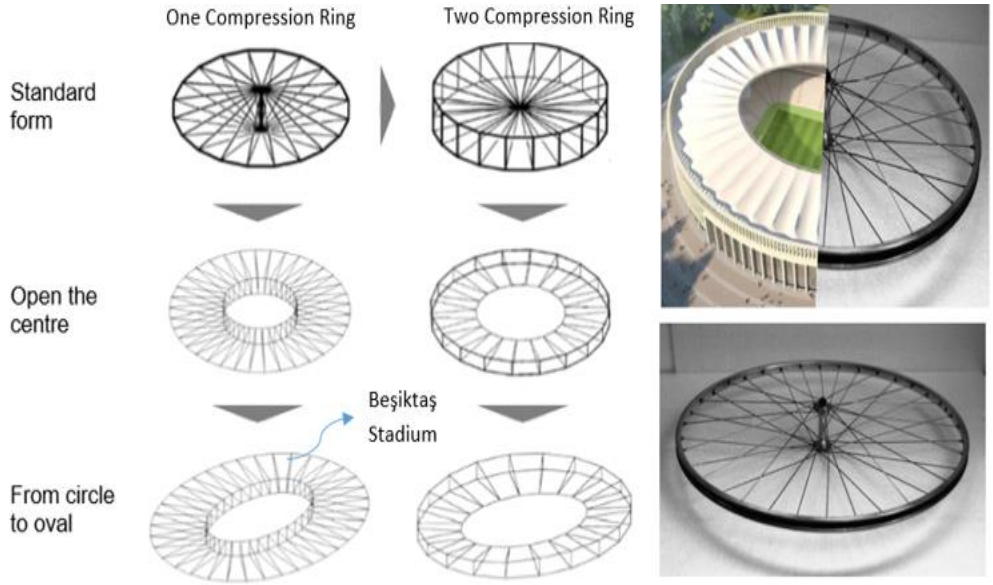

Figure 7. Typical bicycle wheel carrier system applications.

4.Methodology of Structural Modelling

4.1. Analysis Software

The study was carried out with non-linear analysis (GSRelax non-linear) of a model developed with software GSA8.7. It simulates a process of damped vibration in small time cycles. (Oasys Software, web source)

Usually the tension ring is single. However, it can be widely used in systems with double tension ring.

4.2. Numerical Model

4.2.1. Geometry

The geometry for the global model has been created parametrically, optimizing the Compression Ring curvature, Lower Radial variable curvature and bay divisions. All elements are located at the neutral axis of sections, eccentricity between cables work point and inner compression ring, are modeled. No global imperfection is introduced.

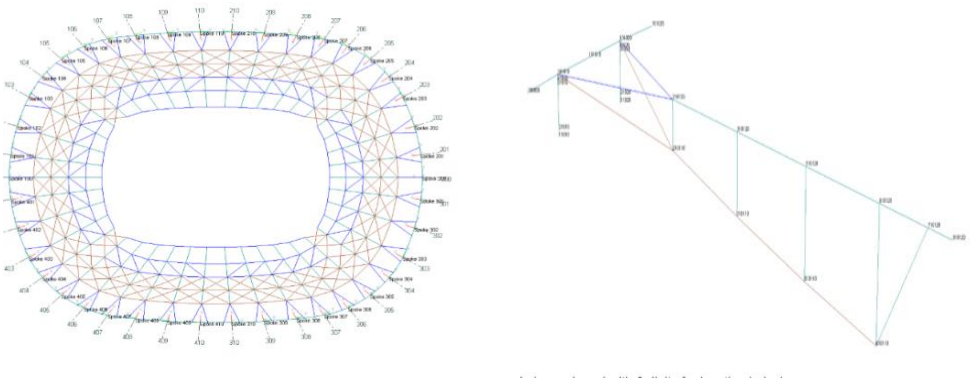

Figure 6. Mathematical model.

4.2.3. Sections and Properties

The listing below shows the section properties used for the global structure model (Table 1).

4.2.3.1. Materials

Table 1. Mechanical properties of the material

N⁰	Name	Type	Young's Modulus [N/mm²]	Poisson's Ratio	Shear Modulus [N/mm²]	Density [t/m³]	αT [1/°C]
M1	Fully Locked Cable	Elastic	155000	0.3	E/2(1+ν)	8	1.2e-5
M2	Steel S355	Elastic	210000	0.3	E/2(1+ν)	8	1.2e-5
M5	Steel S355	Elastic-Plastic	210000	0.3	E/2(1+ν)	8	1.2e-5
M6	Concrete Long Term	Elastic	14000	0.2	E/2(1+ν)	2.4	1.0e-5

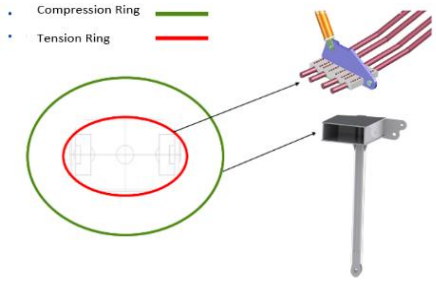

Figure 7. Tension and compression rings.

4.2.3.2. Sections

The following sections have been modeled, including sub-sections used to optimize steel weight:

Table 2. Section properties.

N⁰	Nomenclature	Name	Material	Section [mm]
1	C.R. 1	Compression Ring 1	Steel EC	RHS 600x1400x35x35
2	C.R. 2	Compression Ring 2	Steel EC	RHS 600x1400x35x35
11	F.S. 1	Flying Struts 1	Steel EC	CHS 139.7 x 10
12	F.S. 2	Flying Struts 2	Steel EC	CHS 168.3 x 10
13	F.S. 3	Flying Struts 3	Steel EC	CHS 168.3 x 10
14	D	Diagonals	Steel EC	C 18 (*)
21	F.C.	Flying Columns	Steel EC	CHS 355.6 x 12.5
31	In. S.	Inclined Struts	Steel EC	CHS 219.5 x 12
41	U.R.	Upper Radials	Steel EC	HE300A
42	U.R.	Upper Radials	Steel EC	HE300B
51	L.R. 1	Lower Radials 1	Cable LC	STD C 103 (*)
52	L.R. 2	Lower Radials 2	Cable LC	STD C 75 (*)
53	L.R. 3	Lower Radials 3	Cable LC	STD C 61 (*)
61	U.R.	Upper Radials	Steel EC	HE300B
62	U.R.	Upper Radials	Steel EC	HE300B
63	U.R.	Upper Radials	Steel EC	HE300A
71	U.R. 6	Upper Ring 6	Steel EC	CHS 168.3 x 10
72	U.R. 4	Upper Ring 4	Steel EC	CHS 355.6 x 22
73	U.R. 4	Upper Ring 4 and 3	Steel EC	CHS 355.6 x 12.5
73	U.R. 3	Upper Ring 3	Steel EC	CHS 323.9 x 12.5
81	AT1	Arch Ties 1	Steel EC	CHS 168.3 x 8
82	AT2	Arch Ties 2	Steel EC	CHS 168.3 x 8
83	M. Br.	Membrane Bracing	Cable LC	C 5 (**)
91	U.R.-S.	Upper Split	Steel EC	CHS 323.9 x 12.5
95	L.R.-S.1	Lower Split 1	Cable LC	STD C 75 (*)
96	L.R.-S.2	Lower Split 2	Cable LC	STD C 62 (*)
97	L.R.-S.3	Lower Split 3	Cable LC	STD C 42 (*)
101	L.T.R. 1	Lower Tension Ring 1	Cable LC	STD C 208 (*)
112	H.B.	Horizontal Bracing	Steel EC	CHS 323.9 x 12.5
121	V.B. 1	Flying Bracing 1	Cable LC	STD C 62 (*)
122	V.B. 2	Flying Bracing 2	Cable LC	STD C 62 (*)
151	C. 1	Cuter Columns Lower Part	Steel EC	RHS 280x250x20x50
152	C. 2	Cuter Columns	Steel (***)	CHS 355 x 19
153	C. 3	Columns Upper Part 1	Steel (***)	CHS 355 x 35 (*)
154	C. 4	Columns Upper Part 2	Steel EC	CHS 355 x 35 (*)
201	Mech. Low. 1	Lower Connection 1	Steel EC	C 50
202	Mech. Low. 2	Lower Connection 2	Steel EC	RHS 280x250x20x50

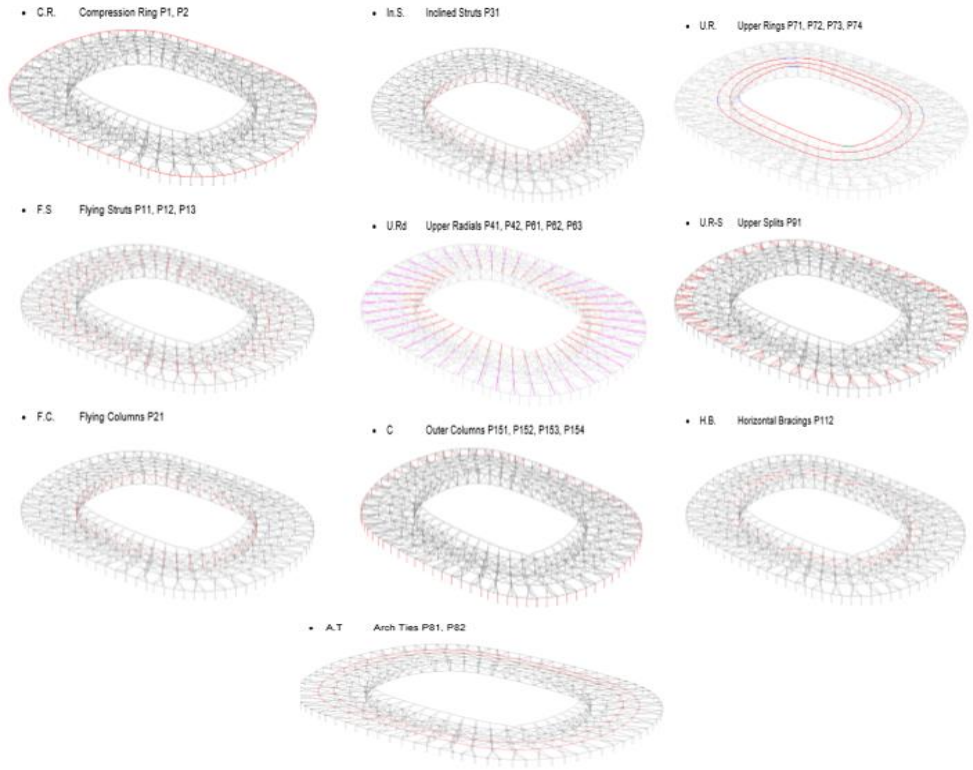

Figure 8. Steel frame elements.

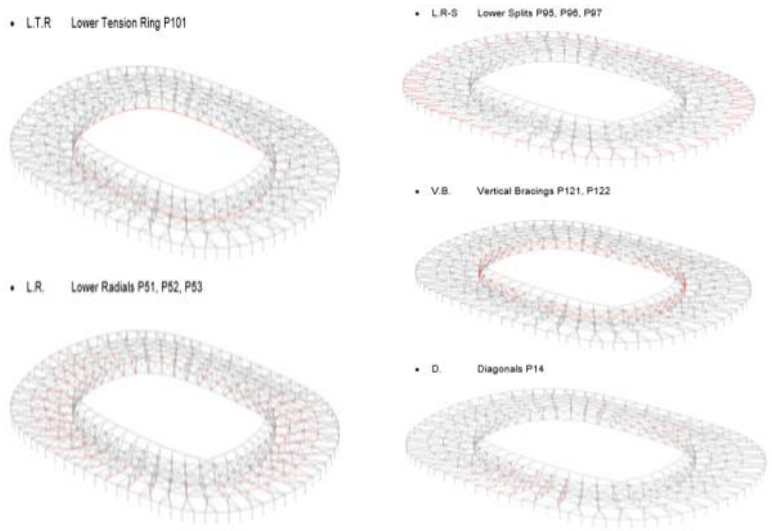

Figure 9. Cable elements.

5. Loads Hypotheses

5.1. Permanent Loads

Density values are in accordance with BS EN1991-1-1: Actions on structures – Densities, self-weight and imposed loads. Steel density is assumed 78.5 kN/m3. Roof cladding weights are described in 5.1.2. Gravity loads are self-weight loads and applied to all elements. Self-weight loads follow the global Z-axis vertically downwards.

5.1.1. Primary Steel Structure

All primary steel structure has been modeled in the structural calculation model, the gravity loads factor was enlarged to 1.1 to cover 10% additional weight from accessories and painting.

5.1.2. Roof Cladding

The stadium roof will be clad with a lightweight pre-stressed membrane; its weight including compression arches and necessary stiffening structure is assumed as 0.10 kN/m^2:
Membrane = 0.013 kN/m; Steel Arches, CHS 193.7x12.5 mm = 0.06 kN/m^2;
Steel Arch Ties, CHS 168 x 8 mm = 0.02 kN/m^2; Edge Cables and fixings = +10 %
No other surface loads (e.g. weight of acoustic or decorative panels) are applied.

5.1.3. Catwalk and Platform

A ring-catwalk along the lower central ring is considered with a permanent uniform load of 2.0 kN/m.
Two radial access bridges are considered with a permanent uniform load of 1.5 kN/m.

5.2. Imposed Loads

5.2.1. Service Loads

The roof structure allows at specific points and along specific axes to receive suspended (or externally applied) service loads. These include:

- Lighting total weight 230 kN, uniformly distributed along the lower central ring (total length 385m ~ 0,6 kN /m).
- Audio service, total weight 275 kN, uniformly distributed along the lower central ring (total length 385m ~ 0,6 kN/m).
- Further equipment and cable weight along catwalk and access walkway 1.5 kN/m
- Video screens, scoreboards 2 x 100 kN, one on each short side, connected to axes 101 201 301 and 401 of the lower central ring.

5.2.2. Additional Equipment Loads

The building user can apply additional technical or decorative equipment to the roof structure (lower central ring TR), e.g. rigging for concerts and shows, via point loads of maximal 5 kN at any of the 42 nodes, respectively as 0.04 kN/m^2. In

conclusion, 3 different set of dead loads are used:

• Dead Load Min = Primary Steel Structure + Cladding + Catwalks

• Dead Load Max = Dead Load Min + Service Loads

• Dead Load Erection = Primary Steel Structure

5.3. Prestress Load

Prestress is a set of forces applied to the main elements (Compression Ring, Lower Tension Ring, Lower Radial Cables, Lower and Upper Splits, Upper Radials), which does not produce any deflection and small bending moment in the Compression Ring. This set of forces is the result of an iterative process:

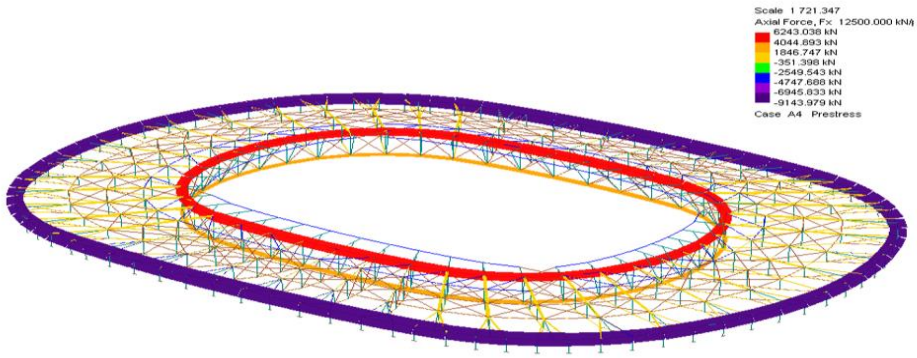

Figure 10. Prestress loads.

5.4. Rainwater Loads

For load and ponding studies, the intensity for 25years of return period is accounted for the design. A minimum slope of 1% at all points and under all circumstances is taken as criteria of acceptance for sufficient rainwater evacuation. Considered peak rain fall values are taken as 4.0 L/sec for 100m².

5.5. Snow Loads

Design ground snow load for Zone II (Istanbul, h<200m) Pk0 = 0.75 kPa (TSE 498)

Slope roof coefficient (angle α=5°) m = 1.00

Design roof snow load Pk = 0.75 kPa

An additional factor of ice build-up of 1.33 is considered, bringing the uniform roof snow load to 1.33 x 0.75 = 1.0kN/m²

Drifted snow shall be considered in the sizing of membrane and supporting elements (arches). Coefficient shall be taken as per Eurocode BS EN 1991-1-3.

For the membrane geometry an angle of max 15° is considered (height 1,5m width of membrane arch 12m) → μ2 ((α1+α2) /2)= 1.2.

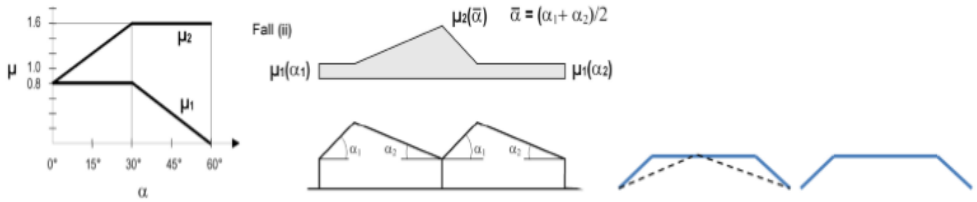

Figure 11. Snow loads on the roof.

The maximum local value of accumulated snow load is 1.2 x 1.33 x 0.75 = 1.2 kN/m².

5 different scenarios are taken into account for the structural calculation:

- Snow uniform and snow uniform exceptional

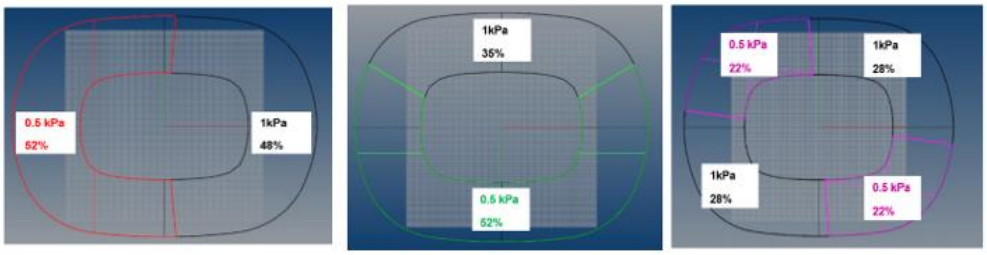

Figure 12. Unbalanced curve side-unbalanced long side-unbalanced unsymmetrical.

Pattern studies have been made to understand the critical unbalanced snow cases.

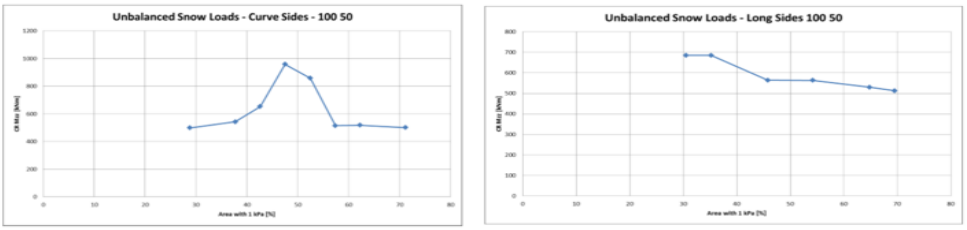

Figure 13. Snow unbalanced loads.

5.5. Thermal Actions

Maximal outside shaded air temperature, Tmax = 41 °C
Maximal outside temperature, taking into account of solar radiation effect, Tout = 41 + 30 = 71°C
Minimal outside shaded air temperature, Tmin = -7 °C
Temperature gradient, ΔT = 13 °C
The total range is 71-(-7) = 78°C. Therefore, in order to be approx. in the middle of this temperature range, the Reference Temperature is T0 = 30 °C. Steel and Cable Suppliers shall take into account workshop temperature during the cutting process of the elements.
4 scenarios of thermal loads are applied:
1. Uniform raise of 41°C on all structure elements.

2. Uniform fall of -37°C on all structure elements.

3. Temperature of all the parts not covered by the membrane (Flying columns) is 13°C higher than exposed steel structure.

4. Temperature of all the parts not covered by the membrane (Flying columns) is 13°C lower than exposed steel structure.

5.6. Supports Movements

The differential movement between adjacent primary concrete blocks due to settlement and expansion joint are considered as:

- ± 30mm in radial direction and tangential direction (60mm in total)
- No differential movement in vertical direction is considered

7 different critical patterns of settlements are considered, respecting the movement joints of the supporting concrete structure:

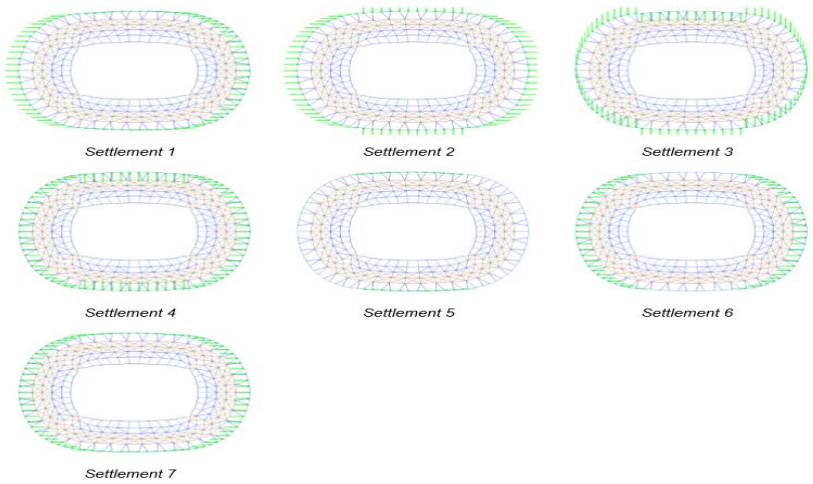

Figure 14. Support Movements.

5.7. Wind Loads

National and related international regulations were used to determine the wind loads affecting the structure. FLUENT fluid finite element analysis program was used for numerical wind tunnel test for the three-dimensional model of the structure since the wind effect is critical for the steel wire rope roof system and these loads are difficult to determine by theoretical methods. In addition, the wind tunnel test was carried out on a small-scale model in Wacker (2013) and the most unfavorable values of realistic wind effects were used in the calculations by checking the Model and Numerical analysis values. It was found.

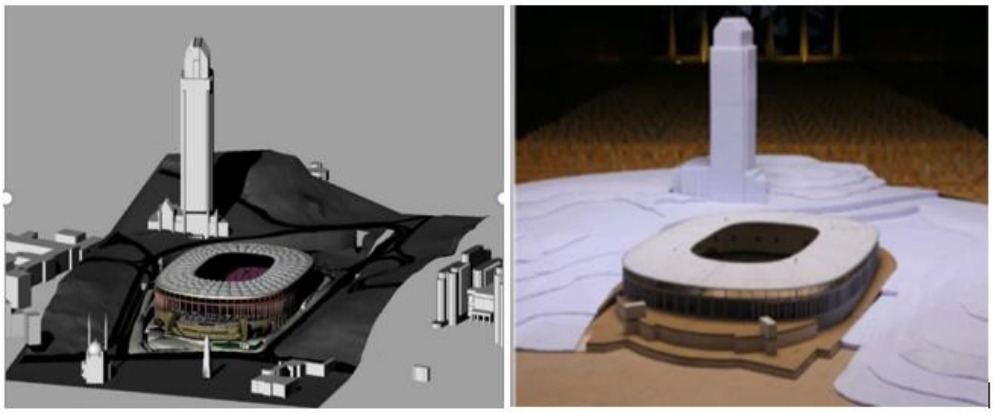

Figure 15. Three-dimensional model of the BJK Stadium and stadium model :1/350 scale.

5.7.1 Computational Fluid Dynamics

Computational Fluid Dynamics or CFD is a numerical algorithm used to solve the partial differential equation known as Navier-Stokes equation:

$$\rho \frac{Dv}{Dt} = -\nabla p + \nabla . T + f. \quad (1)$$

which is a differential form of Newton's 2nd law, incorporating also the law of continuity, i.e. the concept that mass is conserved throughout the volume as the fluid moves, is pressurized, and/or changes density. Here, v is the velocity vector, p is the pressure field, T is the stress tensor and f is the body-force field (such as gravity or electro-magnetic forces). For the simulation of stadium aerodynamics, the following considerations are included in the analysis. ANSYS CFX 15.0 is used to estimate the aerodynamic pressures and wall shear stresses resulting from wind loading at 160 km/h impinging the stadium in the longitudinal (x) and transverse (y) direction.

Air Properties:
Air at 25 C @ Sea Level
Isothermal (no heat transfer)
Turbulence model: scalable k-epsilon
Reference pressure 1 atm:

• ANSYS CFX 15.0 is used to estimate the aerodynamic pressures and wall shear stresses resulting from wind loading at 160 km/h impinging the stadium in the longitudinal direction.

• The geometry is simplified to include a smooth roof for preliminary results, with the structural block near its perimeter which can experience significant pressure from the wind.

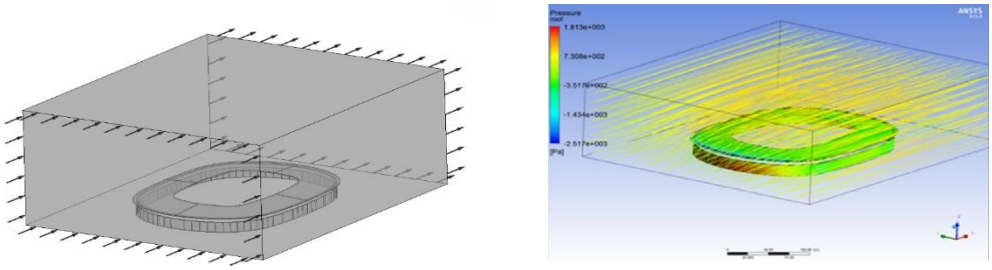

Figure 16. Roof Mesh for finite element methods.

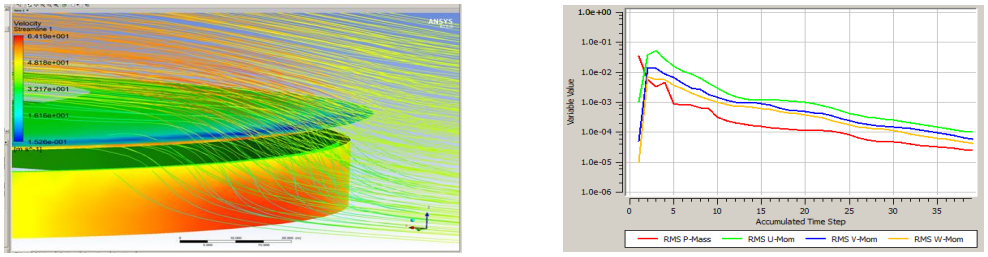

Figure 17. Solution residuals indictaing the error in different variables.

Because of the high-quality mesh, the solution occurs in fewer than 40 iterations. Inflation layers help resolve velocity gradients correctly so the residuals (errors) are reduced quickly and efficiently. The default normalized value of 1e-4 is used as a convergence criterion. (Tello, 2013).

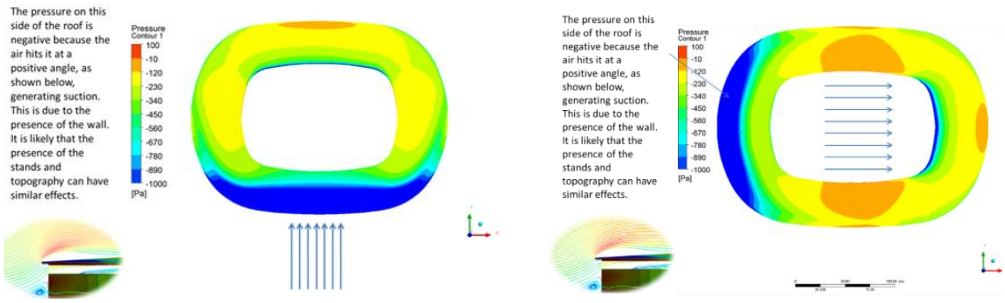

Figure 18. Stress contours on the roof.

5.7.2. Wind Tunnel Test

The extensions of the stadium are about 215 m along the longitudinal axis and about 160 m along the lateral axis. The maximum height of the roof is about 36 m (from the seaside) and about 23 m (landside) respectively. A safe and economic construction and design of the stadium roof of the proposed stadium against wind require the realistic assessment of the structular (area-averaged) peak wind pressures acting on the roof, where both static and dynamic wind loads have to be considered.

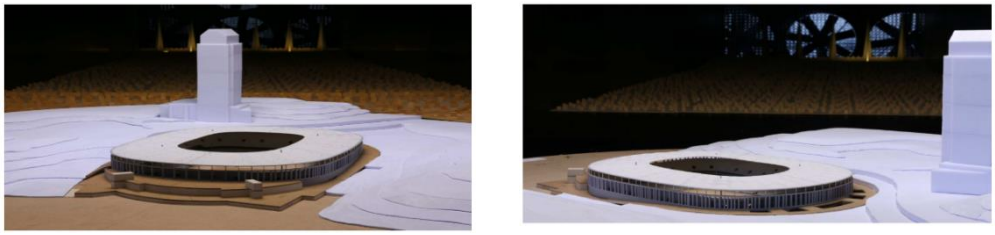

Figure 19. The 1:300 scale model of the stadium in the wind tunnel.

According to the Turkish Code (TS 498, 1997) the gust wind pressure for building heights in between 21 m to 100 m above ground is q = 1.1 kN/m², hence the reference gust wind pressure in stadium height H = 36 m or 23 m respectively would be calculated to : qwİND TSE (H = 36 m / 23 m) = 1.10 kN/m² .The fitted extreme value distribution of the data set leads to the following reference (mean) wind speed for the 50-year return period in 10 m height for open exposure: Vref, 50-years, data = 22.1 m/s. The reference wind speed was also determined as a function of the wind direction. Fig. 22 shows that the highest wind speeds occur at northern wind directions. For other wind directions the calculated reference wind speeds are lower allowing a reduction of the design wind speed (Wacker, 1995; Wacker, 2003).

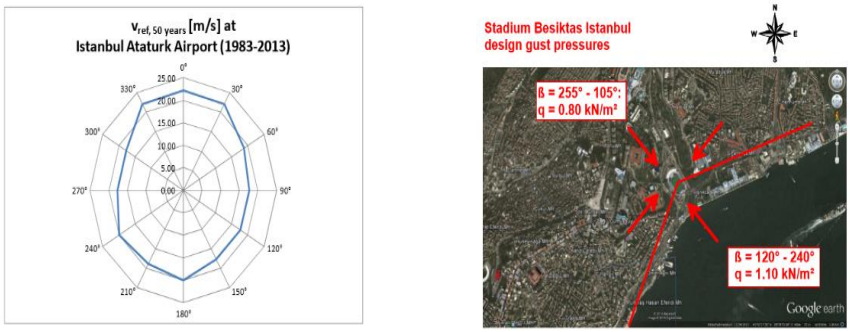

Figure 20. Reference wind speeds (10-min-mean, 10 m height, 50-year return period, open exposure).

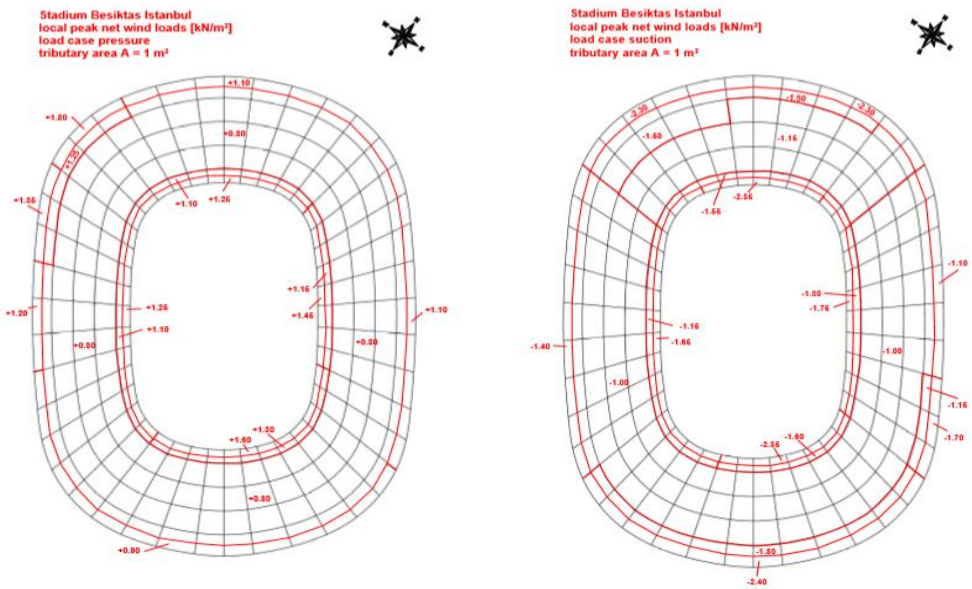

Figure 21. Local peak net wind loads for the design (suction and pressure).

5.8. Seismic Loads

5.8.1. Dynamics Analysis

Based on the information given by the complete model with the Concrete Structure and the Roof Steel Structure has been built:

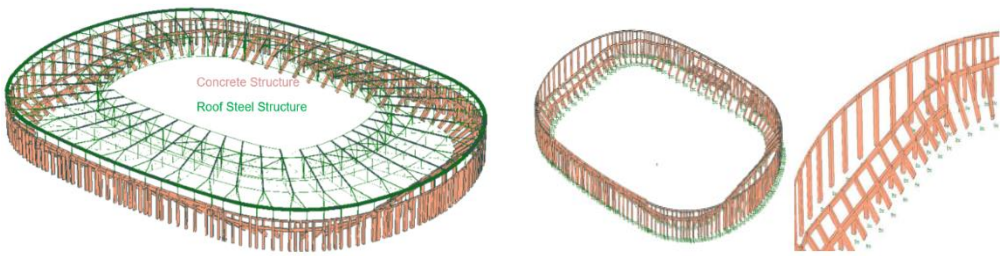

Figure 22. Concrete finite element model.

The following assumptions have been taken: - 119 Concrete Columns fixed at both ends - Concrete Structure fixed at the ends Concrete long term having Young Modulus E = 14000 Mpa

A Ritz P-Δ Modal Analysis has been used as a base for the Response Spectrum Analysis, to include geometric stiffness effects. The P-Δ load case chosen, according to the BS EN 1998-1 3.2.4: DeadLoad max + (Prestress+Geom Compensation) + 0.3 Snow

According to BS EN 1998-1 4.3.3.3 all modes with effective modal masses greater than 5% of the total mass must be taken into account. In order to satisfy this requirement, 100 modes for x, 100 modes for y and 50 modes for z have been considered, where horizontal forces along global X and global Y axes are applied and incremented, monitoring horizontal displacements of the structure. The compared models are:

Table 3. Restraints of the roof column system.

Model Name	Column Lower Connection Radially	Column Lower Connection Tangentially	Lower Mechanism Tangentially (Pin Play)	Column Upper Connection
Model f1	Pin	Fix	Yes	Fix
FIX FIX	Fix	Fix	No	Fix
FIX PIN	Pin	Fix	No	Fix
PIN PIN	Pin	Pin	No	Fix

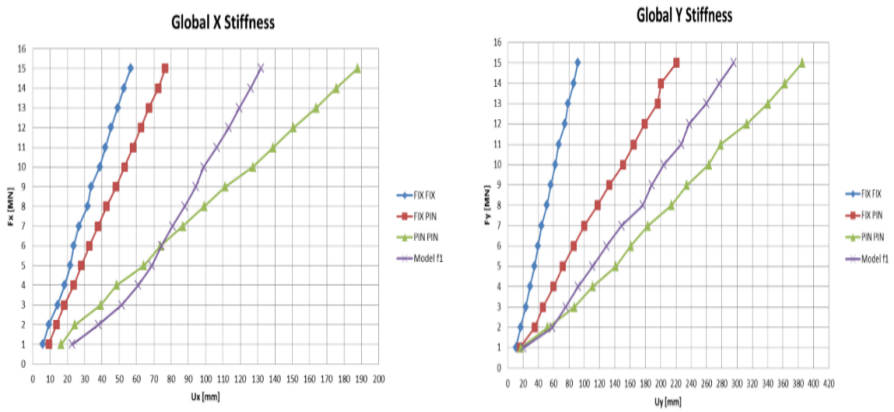

Figure 23. Two directional stiffness diagrams.

Results show that the actual behavior of the structure is between the model "FIX PIN" and "PIN PIN", with horizontal loads higher than 6MN along global X direction and 2MN along global Y direction. Based on this conclusion, the complete model (roof and concrete) includes columns modeled as Model FIX PIN. Being stiffer than Model f1, this approach is more conservative, leading

to higher forces. The coupling effect due to the Concrete substructure has also been studied. A simplified model has been done: The frequency of the lower system has been modified, modifying the stiffness, while the upper system frequency has been kept constant:

Table 4. Summary of the modal values

	Model	M [t]	k [kN/m]	f [Hz]	T [s]
ROOF	A	132	9934	1.38	0.72
CONCRETE	1	13200	572700	1.05	0.95
	2	13200	1328000	1.60	0.63
	3	13200	2038000	1.98	0.51
	4	13200	3371000	2.54	0.39
	5	13200	4722000	3.01	0.33
	6	13200	150900	0.54	1.86
	7	13200	30020	0.24	4.17
	8	13200	1884	0.06	16.67
	9	13200	278300	0.73	1.37
	10	13200	820100	1.26	0.80
	11	13200	1655000	1.78	0.56
	12	13200	2644000	2.25	0.44
	13	13200	4000000	2.78	0.36
	14	13200	5530000	3.26	0.31
	15	13200	7080000	3.69	0.27
	16	13200	16520000	5.63	0.18
	17	13200	32480000	7.89	0.13

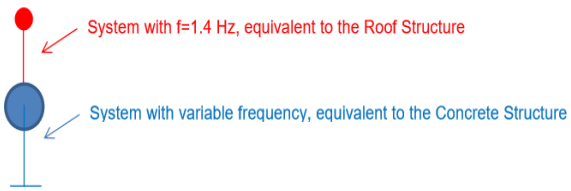

Figure 24. Concrete-Roof structure system frequencies.

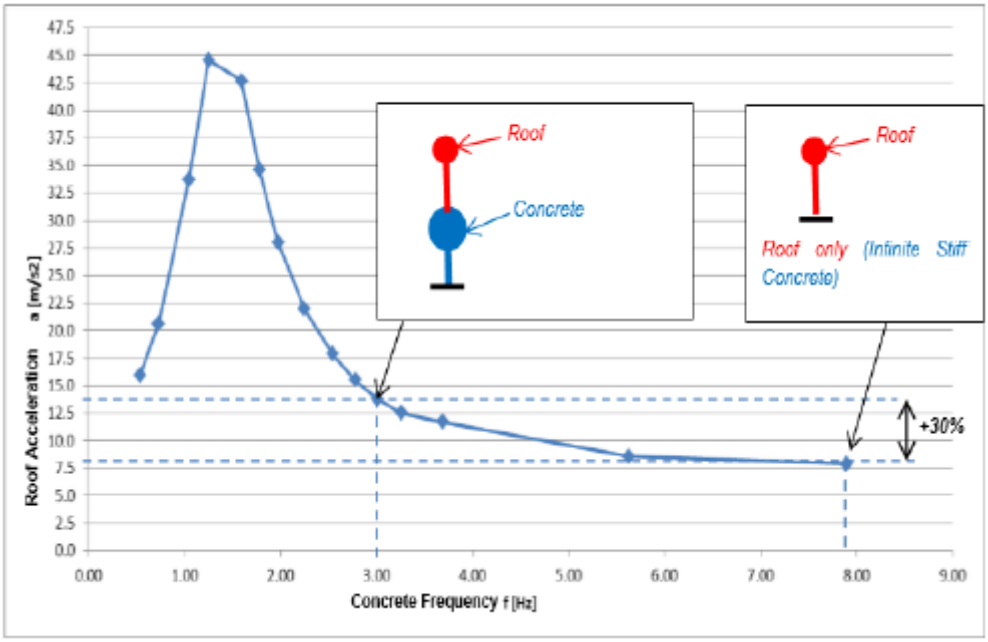

Figure 25. Roof acceleration diagram.

If the Roof Equivalent model is considered alone, i.e. infinite stiff Concrete substructure, the nodal acceleration is 7.4 m/s2: The "Coupling Effect" has an important impact when the ratio $f_{Concrete}/f_{Roof}$ is in the range 1 - 2.5 (the concrete substructure is normally stiffer than the roof structure, therefore its frequency is higher than the roof one). When the Concrete substructure has a frequency of 3 Hz the Roof acceleration increases Roof by 30%, compared to an infinite stiff Concrete substructure.

According to BS EN 1998-1, Table 5. the structure is assumed to be in DCL (Ductility Class Low), having a low dissipative structural behavior: The chosen behavior factor is q = 1.5.

5.8.2. Response Spectrum Analysis

Elastic Acceleration Spectrum is used:

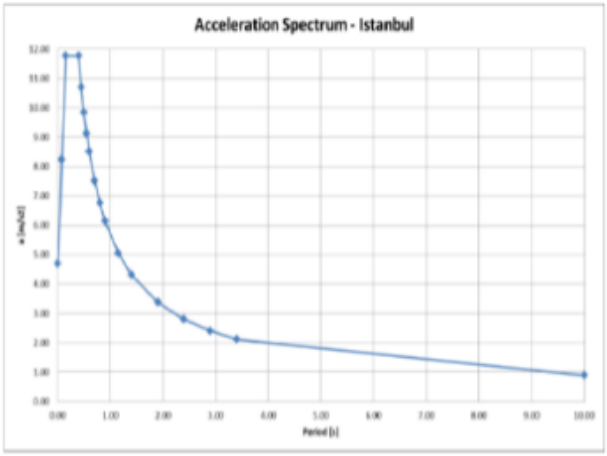

Global Direction	V_{DR+C} [kN]	V_{DR} [kN]
X	11509	9410
Y	7455	7413
Z	5084	3958

Figure 26. Response spectrum curve and base shear force under the earthquake.

Table 5. Ductility behaviour.

Design Concept	Structural Ductility Class	Range of the reference values of the behaviour factor R
Concept a) Low dissipative structural behaviour	DCL	≤1.5-2
Concept b) Dissipative structural behaviour	DCL (Medium)	≤4
	DCL (High)	≤8

Comparing the global forces of the Roof Structure alone and the Roof structure with the Concrete (A B.Y.Y.H.Y., 2007).

5.9. Load Combinations

Load combinations turkey and Eurocode have been completed according to the most unfavorable value.

- Service Limit State (SLS) Combinations: SLS Characteristic combination is used for checking deflection criteria.
- Ultimate Limit State (ULS) Combinations: ULS combination is used for sizing of structural members.

6. Conclusion

The design criteria for Besiktas Stadium were explained and structural information about the stadium structure was given. The design of the stadium structure, including the construction phases, has been a process that requires the co-operation of architectural, design engineers, field engineers, academics and many disciplines in a coordinated manner. The stadium structural system consists of many different bearing elements and the performance of the structure depends on the correct

modeling of the behavior of these elements. Steel construction superstructure Spoke Bicycle wheel technology Steel ring beam pressure ring and Rope Pull ring and main pressure ring on the 82 super-pillars are sitting on and in case of earthquake, a significant amount of horizontal load is transferred from the roof to the super-columns. The roof is 10m with very advanced technology. This type of gabari is a record in the stadium roofs.

7. References

A.B.Y.Y.H.Y. (2007). Turkish Earthquake Code Specification for Buildings to be Built in Seismic Zones. Ankara Official Gazette: Prof. PhD. Aydınoğlu, M.N.

Bergermann, R., & Chlaich, J. (1992). Cable-Membrane Roof for the Arena in Zaragoza, Spain, *Structural Engineering International*, *2*(4), 238-241.

BS-EN. (2001). 1991: Basis of Design and Actions on Structure. London: N. Cook.

BS-EN. (2005). 1990: Basis of Structural Design. Brussels: CEN (Committee Europe Normalisation).

BS-EN. (2005). 1993: Design of Steel Structure. Brussels: CEN (Committee Europe Normalisation).

BS-EN. (2005). 1998: Design Provisions for Earthquake Resistance of Structures. Brussels: CEN (Committee Europe Normalisation).

BS-EN. (2008). 1090-2: Technical requirements for steel structure. London: M. Ogle, G. Bowden.

BS-EN. (2009). 1090-1: Requirements for conformity assessment of structural component. Brussels: CEN (Comitee Europe Normalisation).

Masubuchi, M. (2012). *Conceptual and structural design of adaptive membrane structures with spoked wheel principle-folding to the perimeter*. Germany: Shaker Verlag.

NEHRP. (2004). Recommended provisions for seismic regulations for new Buildings and Other Structures. Newyork: Building seismic safety council national institute of building sciences.

Oasys Software. (2019) *GSA Analysis — Structural Engineering Analysis Software.* Retrieved October 20, 2019, from http://www.oasys-software.com/products/engineering/gsa-analysis.html

Tello, J. S. (2013). *Computational Fluid Dynamic Analysis of New BJK Stadium Roof.* Zinergies-Brasilian.

TSE (1987). 498. Design loads for buildings. Ankara: Technical Comitee.

TSE (1980). 648. Building Code for Steel Structures. Ankara: Technical Comitee.

Wacker, J. (1995). Local Wind Pressures for Rectangular Buildings in Turbulent Boundary Layers. *In Wind Climate in Cities* (pp. 185-207). Dordrecht: Springer.

Wacker, J. (2013). *Besiktas New Stadium wind tunnel testing determination of quasi the structural design of the stadium roof determination of local wind loads for the design of the roof cladding report*. Germany, Wacker Ingenıeur Buroe.

JOURNAL OF JICIVILTECH
INNOVATIONS IN CIVIL ENGINNERING AND TECHNOLOGY

e-ISSN 2687-2129
jiciviltech, 2019, 1(2), 99-105

Research Article/Araştırma Makalesi

Investigating Aluminum Oxide and Silicon Dioxide Modified Bitumen Stiffness Modulus with Empirical Method

*[1]Şebnem KARAHANÇER

[1] *Isparta University of Applied Sciences, Faculty of Technology, Department of Civil Engineering, , Isparta, Turkey, sebnemsargin@isparta.edu.tr, ORCID ID: https://orcid.org/0000-0001-7734-2365*

Geliş / Recieved: 21.12.2019; Kabul / Accepted: 28.12.2019

Abstract

In this study, bitumen was modified with aluminum oxide and silicon dioxide using high shear mixer. As a result of this modification, bitumen performance was investigated with standard test methods. Besides, stiffness modulus and plastic stiffness of bitumen was calculated using empirical methods. Nowadays, nanotubes were used for modification of bitumen, commonly. It is known that, nanotubes can improve the bitumen performance at nano level because of having high specific surface area. Bitumen modification was conducted with aluminum oxide at 3%, 5% and silicon dioxide at 0.3%, 0.5% by weight of bitumen because silicon dioxide has high specific surface area and specific gravity. Bitumen characteristics were determined by bitumen tests (rotational viscometer, penetration, softening point, ductility, elastic recovery and penetration index). In this study, bitumen performance grading (PG) system was used and bitumen was used as PG 64-22. In addition, stiffness modulus and plastic stiffness of bitumen was calculated with empirical methods. As a result, 3% Al_2O_3 and 0.3% SiO_2 modified bitumen has the best performance according to the modification and base bitumen.

Keywords: *Empirical modeling, Stiffness modulus, Plastic stiffness, Bitumen performance, Nanotube modification.*

*[1]Sorumlu yazar / Corresponding author

Bu makaleye atıf yapmak için
Karahançer S. (2019). Investigating aluminum oxide and silicon dioxide modified bitumen stiffness modulus with empirical method. *Journal of Innovations in Civil Engineering and Technology (JICIVILTECH), 1*(2), 99-105.

Alüminyum Oksit ve Silikon Dioksit ile Modifiye Edilmiş Bitümün Rijitlik Modülünün Ampirik Yöntemle İncelenmesi

Öz

Bu çalışmada, bitüm ile alüminyum oksit ve silikon dioksit yüksek devirli karıştırıcı yardımıyla karıştırılarak modifikasyon sağlanmıştır. Bu modifikasyonun sonucunda bitüm performansı standart bitüm deneyleri ile incelenmiştir. Ayrıca ampirik yöntemler kullanılarak rijitlik modülü hesaplanmıştır. Günümüzde nanotüp modifikasyonu yaygın olarak kullanılan bir metot haline gelmiştir. Nanotüplerin yüksek yüzey alanına sahip olmasından dolayı nano boyutta bitüm performansının iyileştirildiği bilinmektedir. Bitüm modifikasyonu ağırlıkça %3, %5 alüminyum oksit ve %0.3 ve %0.5 oranlarında silikon dioksit ile modifiye edilmiştir çünkü silikon dioksitin yüzey alanı ve özgül ağırlığı fazladır. Bitüm karakteristikleri bitüm testleri (dönel viskozimetre, penetrasyon, yumuşama noktası, düktilite, elastik geri dönme ve penetrasyon indeksi) ile belirlenmiştir. Çalışmada bitüm performans derecelendirme (Performance Grade – PG) sistemine göre sınıflandırılmış ve PG 64-22 olarak kullanılmıştır. Ayrıca ampirik yöntemle rijitlik modülü hesaplanmıştır. Sonuçta, 3% Al_2O_3 ve 0.3% SiO_2 modifiye edilmiş bitüm diğer modifikasyonlara göre daha iyi sonuç vermiştir.

Anahtar kelimeler: *Ampirik modelleme, Rijitlik modülü, Plastik rijitlik, Bitüm performansı, Nanotüp modifikasyonu.*

1. Introduction

Nowadays, nanotubes are popular modifiers to improve the bitumen properties because of having high specific surface area and specific properties at nano level. Too many studies have been performed nanotube modification of bitumen. Bitumen properties are improved by nanotube modification. Nano TiO_2, SiO_2, ZnO, CNTs are well-known materials used to modify bitumen in the literature (Hong-liang et al., 2016; Shafabakhsh and Ani, 2015; Nejad et al., 2017). Sadeghnejad and Shafabakhsh (2017) investigated nano TiO_2 and SiO_2 together in different contents (0, 0.3, 0.6, 0.9 and 1.2%) and the results show that different percentages of nano materials is capable to improve the mechanical behavior of stone mastic asphalt, significantly (Sadeghnejad M and Shafabakhsh G., 2017). Zhu, Zhang, Shi and Li (2017) investigated rheological properties of nano ZnO and vermiculite modified bitumen before and after aging. As a result, modified bitumens containing nano modifier showed the lower complex modulus and the higher phase angle (Zhu et al., 2017). Also, carbon nanotubes are usually used nano materials which are comparatively cheap nano material in bitumen modification. Carbon nanotubes can be effectively used to enhance the bitumen rutting performance (Santagata et al., 2012; Arabani and Faramarzi, 2015; Galooyak et al., 2015).

As seen from the literature review there are few study about aluminum oxide modified bitumen and its performance. Also, nano aluminum dioxide was investigated in the literature only by Ali, Ismail, Yusoff, Hassan and Ibrahim (2016) as a modifier of bitumen (Ali et al., 2016). The study indicated that nano AL_2O_3 can be considered as a proper alternative additive to modify the properties of bitumen. This study aims to address the deficiency in the literature. In this study, stiffness modulus and plastic stiffness was calculated with empirical model different from the literature. To this aim, a model was calculated based on Ullidtz and Larsen's mathematical model (Ullidtz and Larsen, 1984). Stiffness modulus and plastic stiffness of bitumen was determined by mathematical model developed by Ullidtz and Larsen (1984). The parameters used are acting time, penetration index and softening point for stiffness modulus. Plastic stiffness was effected by viscosity and the acting time.

In this study, data were taken from previous study (Karahancer et al., 2019). Thus, modification rates were chosen in accordance with the literature. Aluminum oxide and silicon dioxide were added to the bitumen in the rate of 3%, 5% and 0.3%, 0.5%, respectively. High shear mixer was used to modify bitumen with nano materials. Modification effort was conducted at 3000 rpm and at 160 °C degree. After that, rheological tests were conducted on all modified bitumens.

2. Materials and Method

2.1 Materials

60/70 penetration grade bitumen was produced and supplied from Tupras,

İzmir, Turkey. The physical and chemical compositions of the bitumen are listed in Table 1. An aluminum oxide nanoparticle (Al_2O_3) and silicon dioxide nanoparticle (SiO_2) were used in this study as a modifier of base bitumen. Their main properties are listed in Table 2 and Table 3.

Table 1. Bitumen properties

Test		Unit	Base Bitumen
Specific Gravity		gr/cm^3	1.02
Penetration @25 °C		0.1 mm	62.2
Softening Point (Ring & Ball)		°C	49.9
Ductility @25°C, 5 cm/min		cm	>100
RV @135 °C, ≤3Pa.s		Pa.s	0.475
RV @165 °C		Pa.s	0.15
RV @185 °C		Pa.s	0.075
DSR G*/sinδ>1 kPa @10 rad/s	Fail Temperature	°C	67.9
	Grade	°C	64
Mass Loss		%	0
Permanent Penetration		%	70.4
Change in Softening Point		°C	+3.2
DSR G*/sinδ>2.2 kPa @10 rad/s	Fail Temperature	°C	67
	Grade	°C	64
DSR G*.sinδ<5.000 kPa @10 rad/s	Fail Temperature	°C	28.6
	Grade	°C	22
		°C	-12
BBR S≤300 MPa, m≥0.300 @60 s	m-value		0.325
	Stiffness	MPa	213
		Performance Grade	PG 64-22

Table 2. Nano Al_2O_3 properties

Specific Surface Area	≥550 m^2/g
Color and Form	White
Molecular Weight	101.96
True Density	2.9 g/cc
Bulk Density	0.20 g/cc
Al Content (Based on Metal)	>99.1%

Table 3. Nano SiO_2 properties

Specific Surface Area	≥500 m^2/g
Molar mass	60.08 g mol^{-1}
Appearance	Transparent
Density	2.648 g/cm^{-3}
Melting point	1.713 °C
Boiling point	2.950 °C
Purity	99.9%

2.2 Preparation of Modified Bitumen

The modified bitumen was prepared at a temperature of 160 °C. The modifier rates (3% and 5%) of Al_2O_3 and (0.3% and 0.5%) of SiO_2 were added into the base bitumen. The bitumen was mixed at a rate of 3000 rpm for about 90 min using a high shear mixer, in order to acquire the better dispersion of nanoparticles in the base bitumen. Modified bitumen properties were given in Table 4.

Table 4. Nano modified bitumen properties

	0.3% SiO_2 3% Al_2O_3	**0.5% SiO_2 5% Al_2O_3**
Penetration	60.2	65.6
Softening Point	50.9	50.8
Specific gravity	1.025	1.027
Viscosity @135 C	0.654	0.497
Viscosity @165 C	0.13	0.13
Ductility	>100	>100

2.3 Empirical model

Stiffness modulus and plastic stiffness of bitumen was determined by mathematical model developed by Ullidtz and Larsen (Ullidtz and Larsen, 1984). According to Ullidtz and Larsen's stiffness modulus empirical formula, in this study, stiffness modulus of bitumen was calculated. The motivation was to estimate stiffness modulus empirically was to show effect of penetration index on modification.
Ullidtz and Larsen developed a model to determine the stiffness of bitumen given below:

$$S(t) = 1.157x10^{-7}t^{-0.368}e^{-PI}x(T_{rb} - T)^5 \quad (1)$$

where S(t) is stiffness modulus (MPa), t is time for load duration (s), PI is penetration index, T_{rb} is softening point (ring and ball method) (°C) and T is bitumen temperature (°C).

In this model, the time for load duration was calculated from 0.01 s to 0.1 s and the other parameters was calculated from test results (Kuloglu, 2001).

For the plastic stiffness modulus of bitumen was determined as follows (Ullidtz and Larsen, 1984):

$$S(t)_p = 3v/t_a \quad (2)$$

where, $S(t)_p$ is plastic stiffness modulus (MPa), v is viscosity of bitumen (MPa.s), t_a is time for load duration (s).
In this model, the time for load duration was calculated from 0.01 s to 0.1 s and 135 °C viscosity was chosen because the 165 °C and 185 °C viscosity trend was different for modifications (Ullidtz and Larsen, 1984).

3. Results and Discussion

3.1 Penetration Index Results

Penetration Index (PI) was determined to find out the temperature susceptibility of bitumen. Penetration index should be within -1 <PI <+1. As shown in Figure 1, all bitumen has low penetration index value. Best result was obtained with 5% Al_2O_3 and 0.5% SiO_2 modified bitumen.

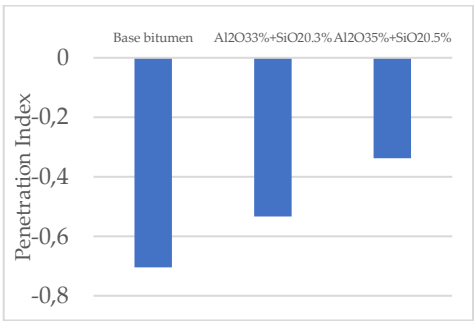

Figure 1. Penetration index values of bitumen

3.2 Viscosity results

The viscosity of the base bitumen becomes greater with the addition of nano Al_2O_3 and SiO_2 at test temperatures (135 and 165°C). However, the 3% and 0.3% modified bitumen samples have shown a significant improvement compared with the base bitumen, as shown in Figure 2. The increase in viscosity is a result of the hardening effect of nano Al_2O_3.

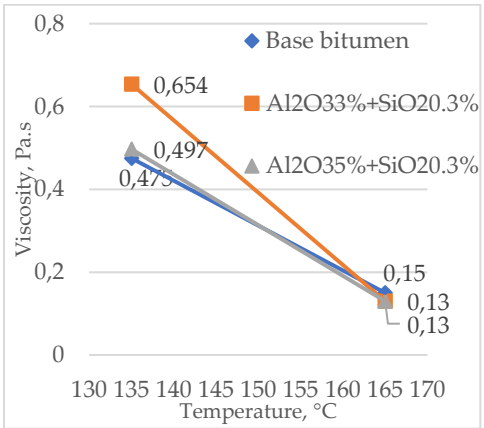

Figure 2. Viscosity values of bitumen

3.3 Empirical Model

Stiffness modulus of Al_2O_3 and SiO_2 modified bitumen was calculated and compared to base bitumen's stiffness modulus. The graph was drawn based on the stiffness modulus of base bitumen (Figure 3). The results showed that 3% Al_2O_3 and 0.3% SiO_2 modified bitumen has the best stiffness modulus better than the base bitumen. All modified samples showed better results when compared to base bitumen.

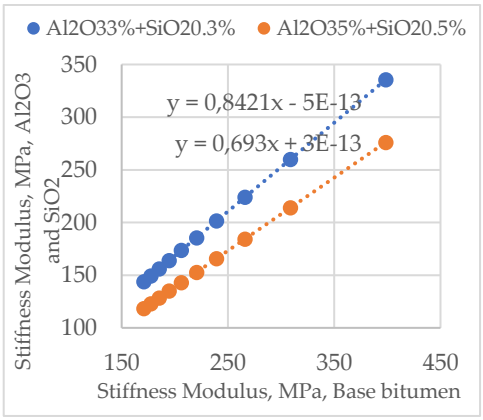

Figure 3. Stiffness modulus of base vs. modified bitumen

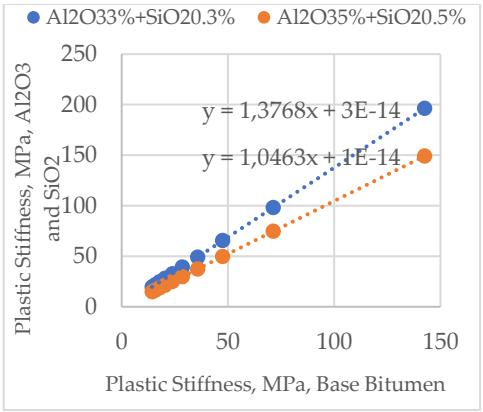

Figure 4. Plastic stiffness of base vs. modified bitumen

Plastic stiffness of Al_2O_3 and SiO_2 modified bitumen was calculated and compared to base bitumen's plastic stiffness. The graph was drawn based on the plastic stiffness of base bitumen (Figure 4). The results showed that 3% Al_2O_3 and 0.3% SiO_2 modified bitumen has the best stiffness modulus better than the base bitumen. Base bitumen has the less plastic stiffness and all modified samples showed better results when compared to base bitumen.

4. Conclusion

In this study, stiffness modulus of Al_2O_3 and SiO_2 modified bitumen was investigated. Bitumen properties and stiffness modulus was determined. Conclusions can be drawn as follows:

According to penetration index, all modifications were in the limit and means that they are less susceptible to temperature than base bitumen. The 3% and 0.3% modified bitumen samples have shown a significant improvement compared with the base bitumen. 3% Al_2O_3 and 0.3% SiO_2 modified bitumen has the best stiffness modulus better than the base bitumen. 3% Al_2O_3 and 0.3% SiO_2 modified bitumen has the best stiffness modulus better than the base bitumen. As a conclusion, 3% Al_2O_3 and 0.3% SiO_2 modified bitumen has the best performance.

5. References

Ali S. I. A., Ismail A., Yusoff N. I. M., Hassan N. A., & Ibrahim A. N. H. (2016). Characterization of the performance of aluminum oxide nanoparticles modified asphalt binder, *Jurnal Teknologi, 78*(4), 91-96.

Arabani M., & Faramarzi M. (2015). Characterization of CNTs-modified HMA's mechanical properties, *Construction and Building Materials, 83,* 207-215.

Galooyak S. S., Palassi M., Farahani H. Z., & Goli A. (2015). Effect of carbon nanotube on the rheological properties of bitumen, *Petroleum and Coal, 57*(5), 556-564.

Hong-liang Z., Man-man S., Shi-feng Z., Yong-ping Z., & Zeng-ping Z. (2016). High and low temperature properties of nano-particles/polymer modified asphalt. *Construction and Building Materials, 114,* 323-332.

Karahancer S., Eriskin E., Saltan M., Terzi S., Akbas M. Y., & Cengizhan A. (2019). Moisture Susceptibility of Nano-Al_2O_3 and SiO_2 Modified Asphalt Mixtures. *International Airfield and Highway Pavements Conference 2019,* 127-135.

Kuloglu N. (2001). Parameters effects the stiffness of bitumen and hot mix asphalt, *Turkish Journal of Engineering and Environmental Science,* 25, 61-67.

Nejad F. M., Nazari H., Naderi K., Khosroshahi F. K., & Oskuei M. H. (2017). Thermal and rheological properties of nanoparticle modified asphalt binder at low and intermediate temperature range, *Petroleum Science and Technology, 35*(7), 641-646.

Sadeghnejad M., & Shafabakhsh G. (2017). Use of nano SiO_2 and nano TiO_2 to improve the mechanical behaviour of stone mastic asphalt mixtures, *Construction and Building Materials, 157,* 965-974.

Santagata E., Baglieri O., Tsantilis L., & Dalmazzo D. (2012). Rheological Characterization of Bituminous Binders Modified with Carbon Nanotubes, *Procedia-Social and Behavioral Sciences, 53,* 546-555.

Shafabaksh G. H., & Ani O. J. (2015). Experimental investigation of effect of nano TiO_2/SiO_2 modified bitumen on the rutting and fatigue performance of asphalt mixtures containing steel slag aggregates, *Construction and Building Materials, 98,* 692-702.

Ullidtz P., & Larsen B. K. (1984). Mathematical model for predicting pavement performance, *Transportation Research Record,* 45–54.

Zhu C., Zhang H., Shi C., & Li S. (2017). Effect of nano-zinc oxide and organic expanded vermiculite on rheological properties of different bitumens before and after aging, *Construction and Building Materials, 146,* 30-37.